



Summer 2018

Interactive effects of ocean acidification and ocean warming on Pacific herring (*Clupea pallasii*) early life stages

Cristina Villalobos

Western Washington University, crisvillalobos926@gmail.com

Follow this and additional works at: <https://cedar.wwu.edu/wwuet>



Part of the [Environmental Sciences Commons](#)

Recommended Citation

Villalobos, Cristina, "Interactive effects of ocean acidification and ocean warming on Pacific herring (*Clupea pallasii*) early life stages" (2018). *WWU Graduate School Collection*. 755.

<https://cedar.wwu.edu/wwuet/755>

This Masters Thesis is brought to you for free and open access by the WWU Graduate and Undergraduate Scholarship at Western CEDAR. It has been accepted for inclusion in WWU Graduate School Collection by an authorized administrator of Western CEDAR. For more information, please contact westerncedar@wwu.edu.

**Interactive effects of ocean acidification
and ocean warming on Pacific herring
(Clupea pallasii) early life stages**

By

Cristina Villalobos

In Partial Completion of
the Requirements for the Degree
Master of Science

ADVISORY COMMITTEE

Chair, Dr. Brooke Love

Dr. Brady Olson

Dr. Leo Bodensteiner

GRADUATE SCHOOL

Gautam Pillay, Dean

Master's Thesis

In presenting this thesis in partial fulfillment of the requirements for a master's degree at Western Washington University, I grant to Western Washington University the non-exclusive royalty-free right to archive, reproduce, distribute, and display the thesis in any and all forms, including electronic format, via any digital library mechanisms maintained by WWU.

I represent and warrant this is my original work, and does not infringe or violate any rights of others. I warrant that I have obtained written permissions from the owner of any third party copyrighted material included in these files.

I acknowledge that I retain ownership rights to the copyright of this work, including but not limited to the right to use all or part of this work in future works, such as articles or books.

Library users are granted permission for individual, research and non-commercial reproduction of this work for educational purposes only. Any further digital posting of this document requires specific permission from the author.

Any copying or publication of this thesis for commercial purposes, or for financial gain, is not allowed without my written permission.

Cristina Villalobos

June 11, 2018

**Interactive effects of ocean acidification
and ocean warming on Pacific herring
(Clupea pallasii) early life stages**

A Thesis
Presented to
The Faculty of
Western Washington University

In Partial Fulfillment
Of the Requirements for the Degree
Master of Science

by
Cristina Villalobos
June 2018

Abstract

The synergy of ocean acidification and ocean warming may lead to negative effects in marine organism responses that would be absent under single stressors. While adult fish are effective acid-base regulators, early life stages may be more susceptible to environmental stressors. Pacific herring are ecologically and economically important forage fish native to the U.S. Pacific Northwest (PNW), and several herring populations in the PNW have experienced reductions in stock abundance. Studies to date have focused on Atlantic herring, and little is known about the response of Pacific herring to ocean acidification and warming. Therefore, this study focused on the combined effects of ocean acidification and warming on Pacific herring early life stages. We incubated Pacific herring embryos under a factorial design of two temperature (10°C, 16°C) and two $p\text{CO}_2$ (600 μatm , 1200 μatm) treatments from fertilization until hatch (11 to 15 days depending on temperature). Elevated $p\text{CO}_2$ was associated with a small increase in embryo mortality. However, elevated temperature was associated with greater embryo mortality, greater embryo heart rates and yolk areas upon hatch, lower percent normal hatch, and decreased larval lengths. The interaction of elevated temperature and $p\text{CO}_2$ was associated greater embryo respiration rates and yolk areas. This study indicates that temperature will likely be the primary global change stressor affecting Pacific herring embryology, and interactive effects with $p\text{CO}_2$ may introduce additional challenges.

Acknowledgments

I thank Dr. Paul Dinnel whose knowledge with Pacific herring assays guided me through the initial fertilization process. I acknowledge my graduate advisor, Dr. Brooke Love, for her support during the entire process and her tinkering expertise when setting up experiments. I would also like to thank my committee members Dr. Brady Olson, who allowed me to work in his research lab, and Dr. Leo Bodensteiner, who provided his expertise in fish biology.

I am also grateful to Dr. Katherina Schoo and Kelley Bright for their assistance in analyzing seawater carbonate chemistry, and general experimental troubleshooting. I also thank Jocelyn Wensloff, Max Miner, Katey Williams, Hillary Thalman, Darby Finnegan, Lynne Nowak, and Tyler Tran for their valuable assistance during experiments.

The Washington Department of Fish and Wildlife was instrumental in providing the specimens for my research. I greatly thank the National Science Foundation, Graduate Research Fellowship Program and Huxley College for financially supporting this research, and assisting with travel expenses to present my work. Lastly, I thank the faculty and staff at the Shannon Point Marine Center for providing support, facilities, and equipment necessary to conduct my research.

Table of Contents

Abstract.....	iv
Acknowledgments.....	v
List of Figures.....	vii
List of Tables.....	ix
Introduction.....	1
Methods.....	9
Results.....	17
Discussion.....	29
References.....	44
Appendix.....	53

List of Figures

- Figure 1.** Groupings of microscope slides based on treatment combinations during the fertilization process. Slide lettering pertains to $p\text{CO}_2$ (first letter) and temperature (second letter). Slide numbering pertains to basin (first number) and female (dashed, second number); R signifies the slide designated for the oxygen consumption experiment. One R slide was placed in each basin. One slide from each female was distributed into each treatment basin.....10
- Figure 2.** Schematic of facility used to conduct tests on Pacific herring larvae. Seawater was continuously pumped from Guemes Channel into the header tank and gravity-fed into 12 mixing tanks. Six of the twelve mixing tanks received pure CO_2 gas ($\sim 1200 \mu\text{atm}$) from a peristaltic pump connected to a CO_2 gas tank – while the other six mixing tanks received untreated seawater ($\sim 600 \mu\text{atm}$). Seawater from the mixing tanks then flowed into 12 treatment basins ($n = 6$ basins at 10°C , $n = 6$ basins at 16°C). Factorial combinations are listed below the treatment basins.....11
- Figure 3.** Examples of a. fertilized (clear membrane around the egg) and b. unfertilized embryos (left panel) (Dinnel et al. 2010), c. dead embryos (middle panel), and d. live embryos (right panel).....13
- Figure 4.** Examples of Pacific herring larvae with no vertebral deformities (top) and larvae with bent vertebral deformities (bottom).....14
- Figure 5.** Averaged $p\text{CO}_2$ values during experiment. Labels within the boxes refer to treatment. Each box represents duplicate samples from each of the three basins per treatment. Whiskers extending from the boxplots indicate standard deviation (SD) from the median (solid black line). Unfilled circles outside the plots indicate outlying data points from the SD.....17
- Figure 6.** Effects of increased $p\text{CO}_2$ and temperature on Pacific herring fertilization success with mean ± 1 SD of 12 measurements. Two-way ANOVA analyses indicate fertilization was not significantly affected by $p\text{CO}_2$ ($F_{1,44} < 0.01$, $p = 0.96$, $\eta^2_p < 0.01$), temperature ($F_{1,44} = 0.01$, $p = 0.90$, $\eta^2_p < 0.01$), or the interaction ($F_{1,44} < 0.01$, $p = 0.98$, $\eta^2_p < 0.01$).....19
- Figure 7.** Pacific herring embryo yolk area for each treatment combination. Data are from images collected over two days before the developing embryo obscured the yolk sac (days 9-10 at 10°C , and 3-4 at 16°C). Data are based on the mean ± 1 SD of (n) measurements: 600:10 ($n = 60$), 1200:10 ($n = 54$), 600:16 ($n = 49$), and 1200:16 ($n = 43$). Two-way ANOVA analyses indicate yolk area was significantly affected by increased temperature ($F_{1,202} = 62.9$, $p < 0.0$, $\eta^2_p = 2.3$) and the interaction of $1200 \mu\text{atm} + 16^\circ\text{C}$ ($F_{1,202} = 7.6$, $p = 0.00$, $\eta^2_p = 0.03$).....19
- Figure 8.** Effects of increased $p\text{CO}_2$ and temperature on Pacific herring normal hatch (A), abnormal larvae (B), and embryo mortality (C). Data represent the mean ± 1 SD of the percentage per slide, where there were 12 slides in the three basins for each treatment. Lower-case letters indicate statistically different treatments based on a Fisher's LSD post hoc comparison.....21

Figure 9. Boxplot depicting embryo oxygen consumption measurements between treatments with and without blank corrections. Each box represents the average rates from six measurements, two vials from each of three basins. Rates are shown as positive values for interpretation.....23

Figure 10. Plots of ambient temperature with $p\text{CO}_2$ (A), and high temperature with $p\text{CO}_2$ (B), on Pacific herring embryo heart rates recorded during one-minute intervals. Recordings occurred on either on day 4 (16°C), or day 5 and 6 (10°C). Data are based on the mean \pm 1 SD of (n) measurements; 600:10 (n = 72), 1200:10 (n = 71), 600:16 (n = 32), and 1200:16 (n = 30).....25

Figure 11. Effects of increased $p\text{CO}_2$ and temperature on the average length (A) and dry weight (B) of Pacific herring larvae. Length data are represented by the mean \pm 1 SD (n) of larvae measurements for 600:12 (n = 414), 600:16 (n = 338), 1200:10 (n = 425), and 1200:16 (n = 271). Weight data are represented by the mean \pm 1 SD (n) of larvae measurements for 600:12 (n = 313), 600:16 (n = 240), 1200:10 (n = 302), and 1200:16 (n = 181). Lower-case letters indicate statistically different treatments based on a Fisher’s LSD post hoc comparison.....27

Figure 12. Average Pacific herring larvae lengths (mm) upon hatch as a function of hatch date and temperature treatment; with $p\text{CO}_2$ pooled within temperature. Blue colored boxplots (10°C treatment) and red colored boxplots (16°C treatment) are separated by the black vertical line, which signifies the time axis for 16°C. The black asterisk indicates the date with the maximum number of live, hatched larvae for both temperature treatments. Regression statistics in the upper plot corners are based on the averaged larval length values for each day.....28

Figure 13. Average Pacific herring larvae dry weights from the max hatch date for both temperature treatments. Data represent values from weigh boats containing 10 or more larvae. Differences between average dry weights were not statistically different ($F_{1,26} = 2.2$, $p > 0.05$, $\eta^2_p = 0.08$).....29

Figure A1. Mean live-hatched Pacific herring larvae during each hatching day for 600:12 (n = 313), 600:16 (n = 240), 1200:10 (n = 302), and 1200:16 (n = 181). Whiskers extending from the boxplots indicate standard deviation (SD) from the median (solid black line). Unfilled circles outside the plots indicate outlying data points from the SD. Treatments are indicated in the upper left corner.....53

Figure A2. The average Pacific herring embryo diameters as a function of treatment groups were measured from development photos taken during the incubation period.....54

Figure A3. Pacific herring embryo development during incubation. Photos are from 2, 4, 6, and 8 days post-fertilization (dpf).....54

List of Tables

- Table 1.** Average in-situ seawater parameters (Orion Star™ A329 pH conductivity meter) and calculated discrete carbonate chemistry values at incubation conditions. Treatments represented by ambient (600 μatm) or high (1200 μatm) $p\text{CO}_2$ cross-factored with ambient (10°C) or high (16°C) temperature with mean \pm 1 SD of (n) measurements.....18
- Table 2.** Two-way ANOVA results for average Pacific herring percent normal hatch (% of live non-malformed larvae/initial embryos), abnormal larvae upon hatch (% malformed larvae/initial embryos), and embryo mortality post-fertilization (% of dead embryos/initial embryos). Data are represented by the mean \pm 1 SD of 12 measurements. * Indicates significance.....20
- Table 3.** Averaged oxygen consumption rates in the blank vials with \pm 1 SD of (n) measurements.....22
- Table 4.** Two-way ANOVA results from the embryo O_2 consumption experiment with and without blank vial corrections. Significance observed in the blank corrected data is likely caused by the variable O_2 consumption rates calculated in the blank vials, and not a treatment effect.....24
- Table 5.** One-way ANOVA results from the embryo heart rate video recordings for both temperature treatments. * Indicates significance.....24
- Table 6.** Two-way ANOVA results for larvae lengths (mm) as a function of hatch date and temperature treatment. * Indicates significance.....28

Introduction

Developing Pacific herring embryos may be negatively affected by environmental change, resulting in decreasing populations (Shelton et al., 2014). Pacific herring in Puget Sound, WA are a key prey item to seabirds, marine mammals, and predatory fish (Stick and Lindquist 2009; Stick et al., 2014). However, herring populations in Washington State have experienced decreasing trends in abundance and spawning biomass by as much as 90% since 1973 (Stick and Lindquist 2009). As such, additional changes in the natural environment may increase stress on Pacific herring populations. This study was the first to investigate near future levels of ocean acidification and warming on Pacific herring early life stages. Findings will help determine their susceptibility to several climate change scenarios, and will provide a better understanding for management and conservation actions.

Ocean Acidification Variability

Atmospheric CO₂ has increased from roughly 280 ppm to nearly 430 ppm since the Industrial Revolution (IPCC, 2014). The oceans have taken roughly a third of this anthropogenic CO₂ (Sabine et al., 2004). This carbon addition causes seawater chemistry to shift towards a decrease in ocean pH and an increase in $p\text{CO}_2$ – a process known as ocean acidification. Climate scientists predict surface seawater pH will decline an additional 0.4 units from pH 8.1 to pH 7.7 by 2100 ($p\text{CO}_2 \sim 1,000 \mu\text{atm}$) (Caldeira and Wickett 2003; IPCC 2014). These predictions for long-term pH changes are primarily modeled for open ocean systems (Duarte et al., 2013). Coastal ecosystems, on the other hand, have a broader range of factors that influence $p\text{CO}_2$. Respiration, eutrophication, and the decomposition of organic matter are interconnected processes that further elevate $p\text{CO}_2$ in coastal systems (Feely et al., 2010; Sunda and Cai 2012;

and Duarte et al., 2013). In addition water entering the Puget Sound via the Juan de Fuca Strait carries the signature of deep $p\text{CO}_2$ -laden seawater upwelled onto Washington coastal shelves during April through November (Feely et al., 2008). Conversely, coastal regions in the Pacific Northwest contain habitats dominated by marine vegetation, such as eelgrass beds, that lower seawater $p\text{CO}_2$ through photosynthetic processes (Duarte et al., 2013; Pacella et al., 2018).

The $p\text{CO}_2$ variability present in coastal ecosystems may enhance or reduce vulnerability of organisms to OA. When anthropogenic acidification is added to periodic, and naturally occurring low pH, the critical pH threshold for organisms' may be exceeded (Hofmann et al., 2010). For example, negative effects of elevated $p\text{CO}_2$ are found in many calcifying organisms (reviewed in Hofmann et al, 2010; Kroeker et al., 2010), where high $p\text{CO}_2$ /low pH results in increased energetic demands for calcification (Venn et al., 2013). Conversely, coastal variability may have caused species to adapt to changing conditions, and they may possess enhanced resilience compared to species from more stable environments (Hofmann and Todgham 2010).

Ocean Acidification and Marine Fish

Organisms with high metabolic activity, the ability to regulate internal pH, and a reduced presence of calcified structures, are hypothesized to be more tolerant to ocean acidification than sessile, calcifying organisms (Pörtner et al., 2005; Wittman and Pörtner 2013). Highly active species, like marine fish, generate excess CO_2 within their tissues and internal fluids through aerobic respiration (Melzner et al., 2009). An accumulation of CO_2 products decreases blood pH, leading to respiratory acidosis (Melzner et al., 2009). To mitigate excess CO_2 in their bloodstream and prevent acidosis, adult marine fish evolved effective acid-base regulation mechanisms (Perry and Gilmour 2006; Deigweier et al., 2008; Heuer and Grosell 2014). During

acid-base regulation, adult marine fish remove excess H^+ ions from their blood plasma through Na^+/H^+ transporters located across gill epithelia (Perry and Gilmour 2006; Deigweiher et al., 2008). Acid-base regulation may additionally be achieved by importing bicarbonate from the environment via epithelial ion transporters to buffer high H^+ concentrations (Deigweiher et al., 2008). Hyperventilation in response to high blood CO_2 is also believed to lessen acidosis by increasing the diffusion of CO_2 across branchial epithelium through greater water flow over their gills (Evans et al., 2005).

Although mechanisms to alleviate acidosis are present in adult fish, fish embryos and larvae lack these acid-base regulation mechanisms. Therefore, early life stages are likely more vulnerable to environmental change (Kikkawa et al., 2003; Ishimatsu et al., 2008). For example, embryos of inland silverside (*Menidia beryllina*), small schooling fish that reside in estuaries along the North American Atlantic coast, were incubated at CO_2 concentrations ranging from 400 μatm to 1100 μatm (representing current ambient conditions to levels predicted for 2100) (Baumann et al., 2011). A week after hatching, a consistent decline in larval survival was observed in embryos reared at 1100 μatm compared to embryos kept at 400 μatm . Olfactory impairment and behavioral changes have been observed in larval orange clownfish (*Amphiprion percula*) at pCO_2 levels above current predictions for this century (2000 μatm) (Munday et al., 2008a). Exposure to ocean acidification conditions hindered larval clownfish from identifying and navigating to suitable settlement sites. Munday et al. (2008a) indicate that this may result in inbreeding among populations because larvae could no longer distinguish between parents and nonparents when choosing settlement sites.

While research has detected negative CO_2 effects in some fish species, other species were robust to elevated CO_2 . For example, Baltic cod (*Gadus morhua*) embryo and larvae

development were not significantly affected by elevated $p\text{CO}_2$ of up to 3200 μatm (Frommel et al., 2012). Hurst et al. (2014) present similar results no effect on growth and hatch rate in embryos of northern rock sole (*Lepidopsetta polyxystra*) when incubated near 1500 μatm . Species-specific responses to ocean acidity are evident rather than a common trend across marine fish (Baumann et al., 2011; Hurst et al., 2013, 2014; Frommel et al., 2014; Hamilton et al., 2017); therefore we cannot predict the response of Pacific herring (*Clupea pallasii*) early life stages.

Pacific herring are forage fish that range geographically along the west coast of North America from Baja California, Mexico to the Bering Sea, and along the coast of Japan (WDFW 2011). In Puget Sound, WA, a semi-enclosed estuary in the U.S. Pacific Northwest (PNW), adult herring spawn in nearshore coastal waters from early spring to mid-summer (Stick and Lindquist 2009).

Variable $p\text{CO}_2$ levels are present in Puget Sound (Feely et al. 2008; Feely et al., 2010). For example, McLaskey et al. (2016) recorded $p\text{CO}_2$ levels ranging between 400 μatm (pH 8.0) and 1600 μatm (pH 7.5), depending on depth (130 – 180 m) within northern Hood Canal. In shallow depths (3 – 5 m) at Friday Harbor, WA, weekly samples from July 2011 to August 2013 showed that seawater $p\text{CO}_2$ was regularly greater than 650 μatm (pH ~ 7.8) (Murray et al., 2015). During early spring to mid-summer months, pH can vary from 7.7 to 8.5 in Padilla Bay, WA (Baumann and Smith 2018). Consequently, Pacific herring embryos may encounter episodic elevation of $p\text{CO}_2$ during development.

Atlantic herring (*Clupea harengus*) may give an insight into how Pacific herring early life stages will respond to ocean acidification. Pacific herring embryos have similar general developmental patterns as those observed in Atlantic herring (Kawakami et al., 2011). Atlantic

and Pacific herring are morphologically similar, but vary geographically and ecologically (Lakkonen et al., 2015). Atlantic herring spawn in North Atlantic waters, where some areas already experience acidified waters ($> 2300 \mu\text{atm}$) (Thomsen et al., 2010). Franke and Clemmesen (2011) reared Atlantic herring embryos under projected $p\text{CO}_2$ levels by 2100 for the Kiel Fjord ($\sim 4000 \mu\text{atm}$), and found no significant malformations or mortality rates compared to control $p\text{CO}_2$ of $480 \mu\text{atm}$. However, newly hatched Atlantic herring larvae had reduced RNA/DNA ratios. RNA concentrations increase as protein synthesis increases and is correlated to growth, therefore examining RNA/DNA ratios allows for detectable changes at a genetic level before noticeable observations occur at higher biological orders. Based on the responses of Atlantic herring it is possible that elevated $p\text{CO}_2$, as a single stressor, may not affect the early life stages of Pacific herring in terms of observable development.

Ocean Warming and Marine Fish

The global mean sea surface temperatures (SST) are projected to increase 3.7°C to 4.8°C by the year 2100 (IPCC 2014). Coastal temperatures for the Pacific Northwest are projected to increase at least 0.5°C , with greater projected warming during the summer (1.9°C to 5.2°C) (Dalton et al., 2013). Temperature influences a range of physiological traits in marine fish. In early developmental stages warmer temperatures accelerate yolk absorption and jaws become functional earlier in several tropical fish species (Fukuhara 1990).

Increased incubation temperature has resulted in shortened embryogenesis and earlier hatching in Atlantic herring and coral reef fish larvae (Johnston et al., 1998; Green and Fisher 2004). In Atlantic herring larvae, the subsequent rate of muscle fiber development was 89% greater at 8°C than at 5°C (Johnston et al., 1998). Although warmer temperatures shorten embryo

ontogeny and accelerate growth, an increased frequency of physical deformities is also observed in these larvae (Vieira and Johnston 1992). Physical abnormalities in the formation of pectoral fins and spinal chords may diminish swimming performance, leading to greater mortality from an inability to capture prey or avoid predators (Vieira and Johnston 1992; Johnston 1993; Johansen et al., 2011; Kawakami et al., 2011).

The development of Pacific herring larvae also depends on rearing temperature. Differences in developmental temperatures may cause irreversible phenotypic changes in early life stages that can negatively affect the growth and survival of later stages (Johnston et al., 1998). Alderdice and Velsen (1971) determined optimal temperature conditions for total hatch, viable hatch, and larvae length to range 5-9°C. Purcell et al. (1990) conducted a field study in southeastern Vancouver Island, where Pacific herring larvae were sampled from 1-5 m depths. They found high densities of abnormal larvae, with vertebral and jaw abnormalities accounting for over 20% of anomalies. High water temperatures in Kulleet Bay (~ 18.2°C) likely stressed the embryos, which affected the development of larvae. In more recent Pacific herring and temperature studies, embryo survival and growth were robust to incubation temperatures between 10°C and 12°C (Dinnel et al., 2007; Kawakami et al., 2011). Temperatures greater than 12°C appear to greatly affect Pacific herring embryo survival. For example, embryo mortality was 50% at 14°C compared with 1% embryo mortality at 12°C (Dinnel et al., 2007). Pacific herring spawn at depths up to 3 m in Puget Sound estuaries. In the Padilla Bay estuary temperatures (from 2002 to 2016) can vary 6.6-16.4°C (Baumann and Smith 2018).

Warming exacerbates oxygen limitation by increasing organism oxygen demand and reducing the solubility of oxygen (Pörtner and Knust 2007). Warmer temperatures may create a mismatch between oxygen demand and the capacity of tissues to obtain oxygen, ultimately

restricting whole-animal tolerance to thermal differences. An organism's capacity to maintain a sufficient oxygen supply is limited by their thermal window, which is dependent on the species and species life stage (Pörtner 2012). From embryo to larval stages, differences in thermal tolerance may relate to a physiological shift in oxygen uptake. Circulatory and ventilations systems become the dominant forms of oxygen uptake in the larval stage, instead of diffusion across the embryo's chorion (Pörtner 2001; Pörtner and Farrell 2008). Under warmer temperatures, greater oxygen demand will likely be observed in Pacific herring embryos.

Stressor Interactions

Investigating single stressors gives an incomplete picture of organism responses since they can be simultaneously exposed to multiple environmental perturbations. Concurrent temperature increases with increasing $p\text{CO}_2$ may cause an additive (both stressors in combination have the same effect as the sum of the single stressor effects), synergistic (combined stressors have greater effect than the sum of the single stressors), or antagonistic (combined effects are lower than the sum of the single stressors) effect. For example, Antarctic juvenile emerald rockcod (*Trematomus bernacchii*) were exposed to three $p\text{CO}_2$ (450, 850, and 1200 μatm) and two temperature (-1 or 2°C) treatments (Davis et al., 2017). The combination of elevated $p\text{CO}_2$ with warmer temperature had an additive effect on juvenile hyperventilation, and Davis et al. (2017) suggest the effect likely served as an acid-base balance mechanism to expel excess CO_2 .

The addition of elevated $p\text{CO}_2$ to high temperature also appeared to have a synergistic effect on oxygen consumption, as the effect was greater than predicted by the response from the single stressors. This additional environmental stressor may reduce the capacity for juveniles to acclimate to warmer temperatures (Davis et al., 2017). Embryos of Antarctic dragonfish

(*Gymnodraco acuticeps*), were incubated under interacting $p\text{CO}_2$ (420, 650, and 1000 μatm) and near-future warming (2°C) conditions (Flynn et al., 2015). Dragonfish embryo mortality was not affected when increased $p\text{CO}_2$ was the sole stressor. However, embryo survival significantly decreased when warming was combined with acidification (420 μatm , $73 \pm 4\%$; 650 μatm , $68 \pm 6\%$; and 1000 μatm , $63 \pm 3\%$).

The responses of Atlantic fish species to multiple stressors were similar to those observed in Antarctic species. A synergistic effect was found, under interacting $p\text{CO}_2$ ($\sim 1600 \mu\text{atm}$) and temperature (22°C) conditions, when 93% of Atlantic flatfish (*Solea senegalensis*) larvae experienced greater skeletal deformities, compared to 2% of affected flatfish larvae in control conditions (400 μatm and 18°C) (Pimentel et al., 2014). In Atlantic cod (*Gadus morhua*), the frequency of larvae with deformities increased with temperature (ranging from 6% at 0°C to 22% at 12°C), and elevated $p\text{CO}_2$ ($\sim 1100 \mu\text{atm}$) had an additive effect, with deformities consistently increasing by as much as 37% at 12°C (Dahlke et al., 2017). In a recent study, Sswat et al. (2018a) assessed Atlantic herring larval survival, size and weight in a factorial design of two temperature (10 and 12°C) and two CO_2 levels (400 μatm and 900 μatm). Under the elevated temperature and CO_2 treatment, larval survival decreased during the experimental period (Table 3, Sswat et al., 2018a). These studies show that interacting temperature and $p\text{CO}_2$ stressors can affect a range of physiological factors depending on life stage and species. Therefore this study was designed to investigate the developmental responses of Pacific herring (*Clupea pallasii*) early life stages under interacting $p\text{CO}_2$ and temperature stressors.

Methods

Sampling Site and Gonad Collections

The Washington Department of Fish and Wildlife (WDFW) collected adult Pacific herring via gill net in May 2017, from documented spawning grounds in Cherry Point, WA (Stick and Lindquist 2009). Gonads from six females and four males were dissected in the field and transported on ice to the Shannon Point Marine Center (SPMC) in Anacortes, WA.

Fertilization Protocol

Fertilization occurred at treatment conditions, 7 h after gonad collections. Two female gonads contained dry and hardened eggs, indicating poor gamete quality (Dinnel et al., 2010); therefore, fertilization occurred with four female gonads, instead of six. Approximately 50 – 100 eggs were lifted from an ovary using a micro-spatula and dispersed onto groups of four glass microscope slides (25 x 75 x 0.1 mm) under temperature and $p\text{CO}_2$ treatment combinations. Testis samples ($\sim 1 \text{ cm}^3$) from each male were combined and macerated using razor blades in one of four 200 mL bowls representing the treatment combinations. A 1 mL aliquot of the homogenized sperm suspension was used to fertilize each set of microscope slides. After a ten-minute period embryos were adhered to the slides, and were gently rinsed with their respective treatment water to remove sperm and ovarian remnants.

This process occurred 3 additional times for the other females (Fig. 1). Individual slides were placed inside 200 mL glass bowls and photographed to determine initial counts (Stereomicroscope: Olympus SZ40, 6.7x magnification; Camera: Nikon DSLR D3300 55mm lens). Five slides were distributed to each respective treatment basin, four slides for embryo measurements and one slide was used for the oxygen consumption experiment. To account for maternal variability, each treatment basin contained embryos from one of the four females.

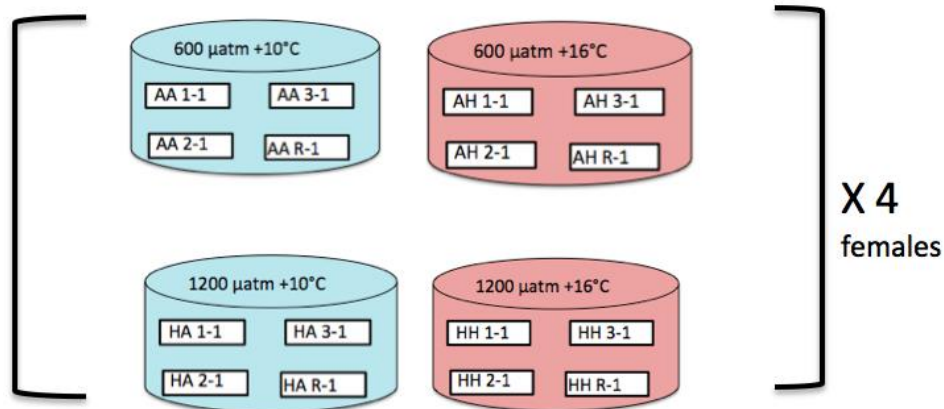


Figure 1: Groupings of microscope slides based on treatment combinations during the fertilization process. Slide lettering pertains to $p\text{CO}_2$ (first letter) and temperature (second letter). Slide numbering pertains to basin (first number) and female (dashed, second number); R signifies the slide designated for the oxygen consumption experiment. One R slide was placed in each basin. One slide from each female was distributed into each treatment basin.

Experimental Setup

Embryos were incubated in a triplicated 2 x 2 factorial framework consisting of two water temperature (10°C , 16°C), and two $p\text{CO}_2$ treatments ($600 \mu\text{atm}$, pH 7.8; $1200 \mu\text{atm}$, pH 7.5). A header tank (170 L) received filtered seawater drawn from Guemes Channel 7 m below mean lower low water. Seawater was aerated with ~ 10 air stones within the header tank, to ensure good oxygenation and bring CO_2 to atmospheric equilibrium, before being gravity fed into twelve, 40 L mixing tanks at 4 L min^{-1} (Fig. 2). Within each mixing tank, submersible power head pumps (Marineland Maxi-jet 900) circulated water using magnetically driven impellers. Six pumps continuously received CO_2 gas (40 mL min^{-1}) from an 8 channel Masterflex[®] L/S Digital Drive (model UX-77921-75) peristaltic pump attached to a 20lb food grade CO_2 gas cylinder with a regulated output of 10 psi. The pumps broke up the CO_2 gas into miniscule bubbles, which quickly dissolved within the mixing tanks (after Jokiel et al., 2014).

Clear acrylic sheets ($5/8''$) covered the 12 treatment basins ($n = 3$ basins per treatment) to

reduce gas exchange. Water flow from the mixing tanks into the treatment basins was gravity fed through tubing restricted to 1/16" ID at the lower end. The basin volume (11 L) and water flow rate into the basins (3.6 mL s^{-1}) allowed for a residence time (50 min) that permitted the 100 W submersible resistance heaters (Aqueon® Submersible Aquarium Heater) to raise the ambient seawater temperature (10°C) to 16°C in half of the basins. Each basin housed 200 mL glass bowls containing the developing embryos ($n = 5$ bowls per basin). Bowls were covered with fine mesh to allow water to circulate but prevent escapement of hatched larvae. Water circulation pumps (Hydor Koralia Nano 240) ensured uniform temperatures within the basins, and standpipes within the basins and tanks allowed excess seawater to flow to waste.

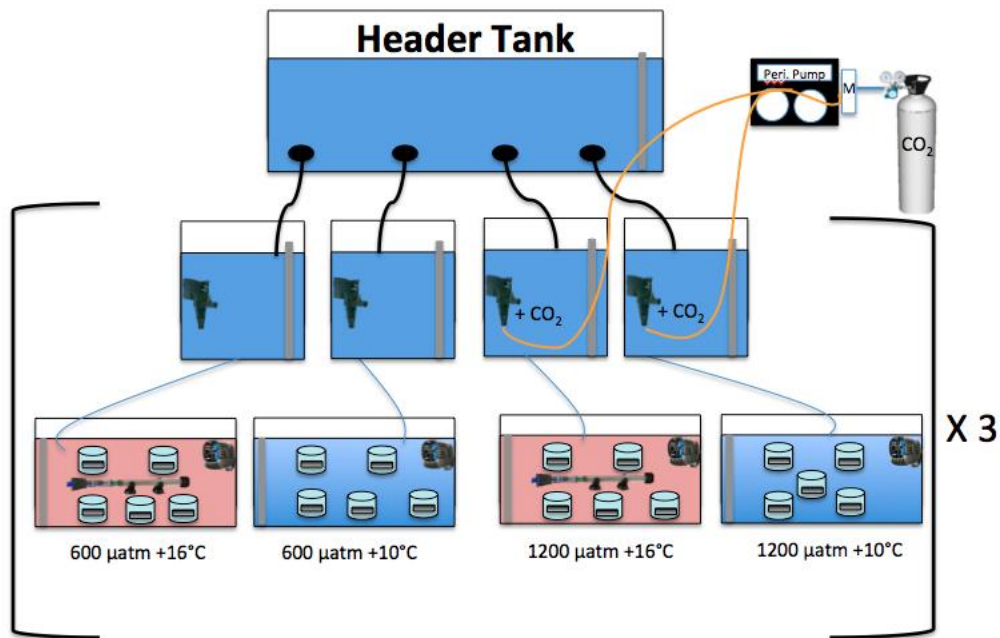


Figure 2: Schematic of facility used to conduct tests on Pacific herring larvae. Seawater was continuously pumped from Guemes Channel into the header tank and gravity-fed into 12 mixing tanks. Six of the twelve mixing tanks received pure CO_2 gas ($\sim 1200 \mu\text{atm}$) from a peristaltic pump connected to a CO_2 gas tank – while the other six mixing tanks received untreated seawater ($\sim 600 \mu\text{atm}$). Seawater from the mixing tanks then flowed into 12 treatment basins ($n = 6$ basins at 10°C , $n = 6$ basins at 16°C). Factorial combinations are listed below the treatment basins.

Carbonate Chemistry

Daily temperature and pH values were recorded using a hand-held, Orion Star™ A329 pH conductivity meter calibrated with NBS-buffers at 10°C. Basin seawater samples were drawn on days 2, 7, and 12 for carbonate chemistry analyses. Samples were passed through a 0.6 µm glass fiber filter before filling 20 mL scintillation vials for duplicate pH and duplicate dissolved inorganic carbon (DIC) samples. DIC samples were poisoned with 10 µL of mercuric chloride (HgCl₂), refrigerated at 2°C, and analyzed a week after collection. A DIC analyzer (Apollo SciTech AS-C3) extracted 2 – 5, 0.75 mL subsamples from the vials. If the first two subsamples were within a 2-µmol kg⁻¹ range of each other, the instrument proceeded to the next sample. If the two subsamples were outside the range, up to 3 additional subsamples were extracted. Room temperature and sample salinity (measured with refractometer) were used to calculate density and convert DIC measurements between µmol L⁻¹ and µmol kg⁻¹. DIC values were calibrated against a standard curve, calculated from the area of five varying volumes of certified reference material (CRM, Batch 149, Dickson, Scripps Institute of Oceanography).

Seawater samples for pH measurements were not poisoned, and were analyzed within a few hours of collection. A diode array spectrophotometer (Agilent 8453A UV-VIS) was used to quantify pH. Basin seawater samples were kept in a 25°C water bath before transferring, via syringe, into a jacketed 5 cm cuvette. The samples received one 30-µL aliquot of *m*-cresol indicator dye to determine the absorbance at three wavelengths (730 nm, 578 nm, and 434 nm) (Dickson et al., 2007). Both DIC and pH measurements were used to calculate *p*CO₂, pH (total scale), and aragonite saturation states (Ω) using CO2SYS (Lewis and Wallace 1998) with K₁ and K₂ equilibrium constants refit by Dickson and Millero (1987). Mixing tank salinity was measured during carbonate chemistry sampling, using a hand-held YSI instrument (Model 85).

Data Collection

Fertilization Success and Normal Hatch

The presence of a raised membrane around the embryo indicated successful fertilization (Fig. 3a, 3b, Dinnel et al., 2010). Dead embryos post-fertilization (Fig. 3c) were recorded from the slides every 24 hours until all individuals had hatched or died. Dead embryos were removed from the slide when not attached to a live embryo (Fig. 3d). When hatching commenced, daily counts of abnormal, dead, and live larvae were recorded (Fig. 4). Live, non-malformed larvae were collected and immersed in a 10 mL bath of tricaine methanesulfonate (MS-222) at a concentration of 250 mg L⁻¹ of seawater. Anesthetized larvae – unresponsive to physical stimuli – were euthanized in a 5% formalin solution and preserved with 15 mL of 200-proof ethyl alcohol in high-density polyethylene vials. Percent normal hatch was determined by counting the number of live, non-malformed larvae versus the initial number of fertilized embryos.

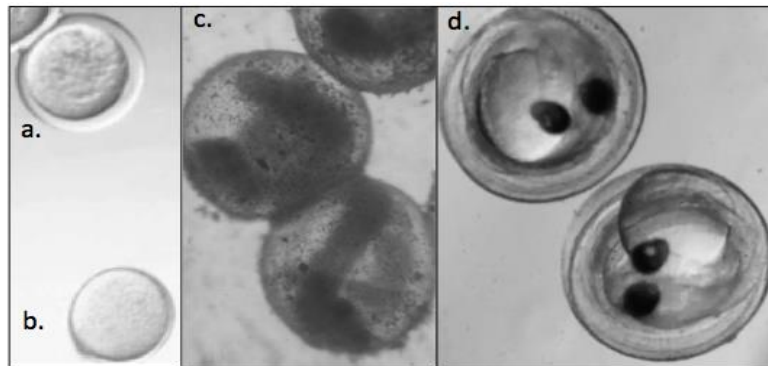


Figure 3: Examples of a. fertilized (clear membrane around the egg) and b. unfertilized embryos (left panel) (Dinnel et al. 2010), c. dead embryos (middle panel), and d. live embryos (right panel).

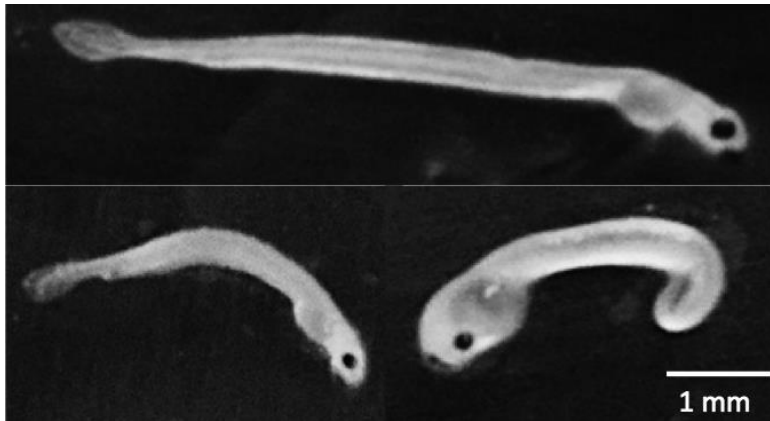


Figure 4: Examples of Pacific herring larvae with no vertebral deformities (top) and larvae with bent vertebral deformities (bottom).

Development, Yolk Areas, Oxygen Demand, and Heart Rate

Beginning on day 2, three embryos from each slide were haphazardly chosen by marking the underside of the slide to observe development. Chosen embryos were photographed daily using identical camera and microscope settings from fertilization. Embryo yolk areas were measured from two days of digital photographs taken before the developing embryo obscured the yolk sac (days 9-10 at 10°C and days 3-4 at 16°C). Yolk areas were measured using the oval tool in ImageJ. Heart visibility depended on embryo development stage and position. Video recordings of embryo heart rates occurred on day 4 and days 5-6 for the 16°C and 10°C treatment, respectively. One-minute videos from haphazardly selected embryos from each slide in the basins ($n = 62$ videos at 16°C, and 143 videos at 10°C), by angling a 55mm Nikon D3300 lens into an Olympus SZ40 Stereomicroscope viewfinder (6.7x). Embryos at 16°C were further along in development than embryos at 10°C (Appendix A, Fig. A3) when videos were recorded. Therefore a direct comparison across all treatments cannot be made, so heart rate data were analyzed separately by temperature groupings. Heart rates were visually counted during video analysis.

In addition to video recordings, we measured embryo oxygen consumption rates using a Microx TX3 oxygen meter (PreSens GmbH, Germany) connected to a polymer optical fiber. We placed 10 haphazardly chosen embryos from one slide into glass vials (2 mL) with micro-optode sensor spots (n = 2 vials per basin, 6 vials per treatment). Vials were overflowed with treatment water to eliminate headspace, capped, and aligned in holders floating inside a 10°C or 16°C basin. Recordings were taken every 30 minutes, until vials experienced a ~20% drawdown in oxygen saturation, for a total of 3 hours. Vials were carefully inverted by hand every fifteen minutes, and right before measurements, to disperse oxygen gradients that may have formed around the embryos. For blank measurements, vials were only filled with treatment water and recorded simultaneously as the embryo filled vials (n = 1 blank vial per basin, 3 per treatment).

Measurements beginning 30 min after vials were filled were used to calculate rates. Oxygen consumption rates were calculated as the slope of the regression line between O₂ concentration (mg L⁻¹) and time (min). Embryo oxygen rates were corrected for background oxygen consumption by subtracting the regression slope of the corresponding blank vial, and data were normalized by the number of embryos (n = 10) in each vial.

For six vials in the 600 µatm +16°C treatment, only raw data (phase angle) were recorded. A 2nd order polynomial equation ($r^2 = 0.99$) was derived from the other calibrated, 16°C vials relating phase angle (deg.) and oxygen (mg/L) values. The equation was then used to derive oxygen concentrations using the phase angle values from the six vials.

Larval Morphology at Hatch

The number of larvae per sample varied depending on daily hatch numbers, but only samples with ≥ 10 larvae were analyzed for dry weight measurements because the scale precision

was not sufficient for smaller samples. We placed larvae samples on aluminum boats (2 in x 1 in) for drying and weighing. Empty weigh boats (n = 58 total) were desiccated in a 70°C drying oven for at least 24 hours, and weighed on a Mettler Toledo™ AB135-S/Fact analytical scale to the nearest 0.01 mg. Larvae were drawn from the vials, placed on a Petri dish, and rinsed with deionized water. Excess liquid was removed and larvae were carefully transferred to a labeled aluminum dish. Larvae were photographed with the Nikon D3300 DSLR 55mm lens that was positioned on a custom platform 11 cm above the dish. Larvae were dried at 70°C for 24 hours minimum, and reweighed on the analytical scale to determine dry weight. Initial boat weights were subtracted from the final weights, and divided by the number of larvae on the boat, yielding mean dry weight (DW) per fish larva. Digital photographs were analyzed using the segment tool in ImageJ to measure larval standard length (from the tip of the snout to the last vertebrae) to the nearest 0.1 mm, by placing a ruler adjacent to the weight boat.

Statistical Analysis

Fertilization success, yolk area, percent normal hatch, embryo heart rates, and larval morphology (average length and dry weight) data were expressed as means \pm standard deviations. All of the above mentioned data were tested for equal variance and normality using Levene's and Shapiro-Wilk methods, respectively, before using a multifactorial analysis of variance (two-way ANOVA) to evaluate the effects of temperature and $p\text{CO}_2$ (fixed factors), or the interaction of factors. Fisher's LSD post hoc comparisons were used to detect significant differences between the means. Statistical significance was determined by $p \leq 0.05$. All statistical testing was conducted using R software (R Developmental Core Team, version 3.1.2, 2014).

Results

Incubation Conditions

Ambient (600 μatm) $p\text{CO}_2$ conditions remained fairly constant over time (Fig. 5). The ambient $p\text{CO}_2$ was slightly higher than the “current-day” ~ 400 μatm of $p\text{CO}_2$ used in recent studies (Miller et al., 2015; Dahlke et al., 2016; Davis et al., 2017). The high (~ 1200 μatm) $p\text{CO}_2$ treatments showed greater variability between and within days (Table 1), but the total DICs for the two high $p\text{CO}_2$ treatments were not statistically different from each other ($F_{1,15} = 0.6$, $p > 0.05$, $\eta^2_p = 0.03$).

This implies outgassing of CO_2 was not an issue at 16°C . The $p\text{CO}_2$ and pH differences between the 1200 $\mu\text{atm} + 10^\circ\text{C}$ and 1200 $\mu\text{atm} + 16^\circ\text{C}$ occurred from the warmer temperature shifting the chemical equilibrium towards an increase in H^+ ions. The higher $p\text{CO}_2$ at 16°C is also due to the solubility of CO_2 decreasing with increasing temperature. Although both elevated $p\text{CO}_2$ treatments have the same total DIC, the 16°C basin was in equilibrium with a higher atmospheric $p\text{CO}_2$ because of the lower solubility. Temperature values averaged to 10.4°C in the ambient basins and 16.2°C in the high basins. Salinity remained stable across basins (Table 1).

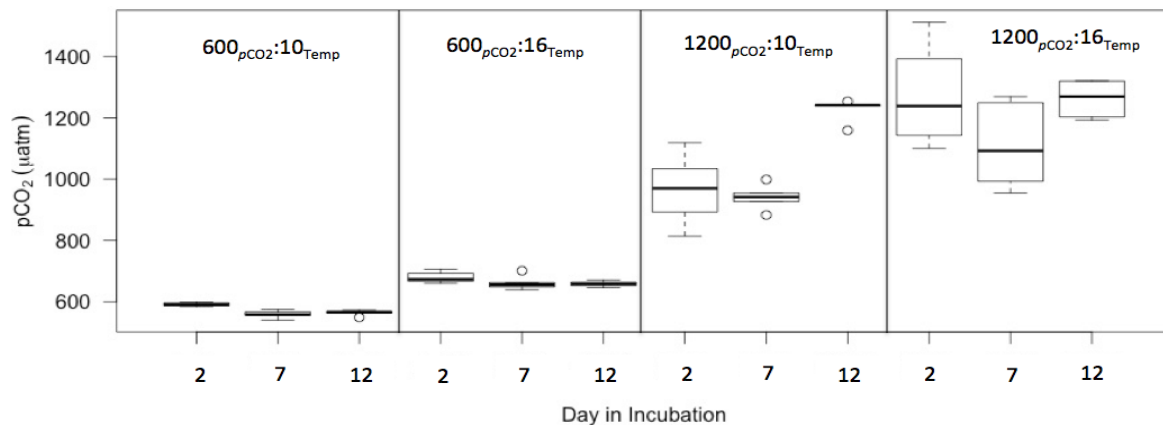


Figure 5: Averaged $p\text{CO}_2$ values during experiment. Labels within the boxes refer to treatment. Each box represents duplicate samples from each of the three basins per treatment. Whiskers extending from the boxplots indicate standard deviation (SD) from the median (solid black line). Unfilled circles outside the plots indicate outlying data points from the SD.

Table 1: Average in-situ seawater parameters (Orion Star™ A329 pH conductivity meter) and calculated discrete carbonate chemistry values at incubation conditions. Treatments represented by ambient (600 μatm) or high (1200 μatm) $p\text{CO}_2$ cross-factored with ambient (10°C) or high (16°C) temperature with mean \pm 1 SD of (n) measurements.

In-Situ Measurements				Discrete Samples		
Test $p\text{CO}_2$ ($\mu\text{atm} + ^\circ\text{C}$)	pH (NBS Scale)	Temperature ($^\circ\text{C}$)	Salinity (PSU)	$p\text{CO}_2$ (μatm)	DIC ($\mu\text{mol kg}^{-1}$)	pH (Total Scale)
600 +10	7.92 \pm 0.03 (47)	10.4 \pm 0.03 (47)	28.9 \pm 0.05 (3)	572 \pm 17 (18)	1946 \pm 13 (18)	7.87 \pm 0.01 (18)
600 +16	7.87 \pm 0.03 (42)	16.1 \pm 1.5 (42)	28.8 \pm 0.15 (3)	666 \pm 18 (18)	1942 \pm 12 (18)	7.81 \pm 0.01 (18)
1200 +10	7.60 \pm 0.06 (48)	10.4 \pm 0.03 (48)	28.3 \pm 1.0 (3)	1034 \pm 145 (17)	2004 \pm 20 (17)	7.63 \pm 0.06 (17)
1200 +16	7.58 \pm 0.04 (42)	16.4 \pm 1.0 (42)	27.3 \pm 0.60 (3)	1221 \pm 138 (17)	2000 \pm 12 (17)	7.57 \pm 0.05 (17)

Fertilization, Development, and Normal Hatch

Embryo yolk area, percent normal hatch, and embryo mortality changed under elevated temperature and/or $p\text{CO}_2$, while fertilization success was greater than 80% in all dishes and was not affected by the treatments (Fig. 6). Higher temperature was associated with increased embryo yolk areas by 14% between the 10°C to 16°C treatment (Fig. 7). The stressor interactions had an additional effect on embryo yolk areas with 26% larger areas in the 1200 μatm +16°C treatment than in the ambient 600 μatm +10°C treatment (Fig. 7). The warmer temperature treatment reduced the average percent normal hatch from 66% at 10°C to 32% at 16°C (Table 2). Therefore increased temperature decreased normal hatch by an average of 34% (Fig. 8A). The proportion of larvae hatched with abnormalities did not differ among any of the treatments and averaged 17% overall (Table 2, Fig. 8B). Embryo mortality post-fertilization significantly increased from 16% at 600 μatm +10°C to 42% at 600 μatm +16°C, increasing mortality by 26%. The $p\text{CO}_2$ had a significant effect on embryo mortality, which increased from 16% at 600 μatm +16°C to 58% at 1200 μatm +16°C (Fig. 8C, Table 2).

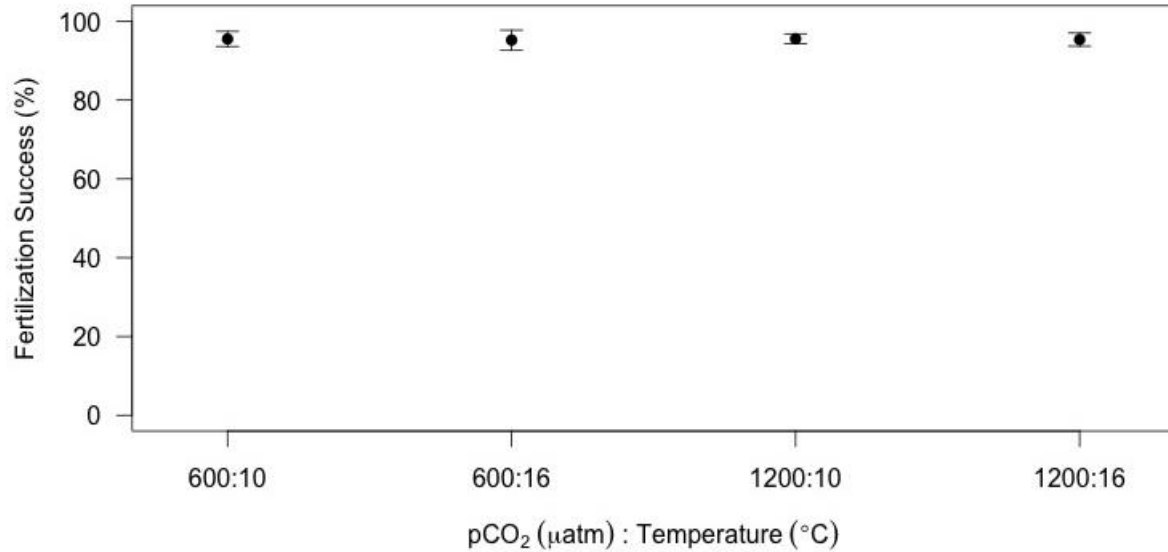


Figure 6: Effects of increased $p\text{CO}_2$ and temperature on Pacific herring fertilization success with mean \pm 1 SD of 12 measurements. Two-way ANOVA analyses indicate fertilization was not significantly affected by $p\text{CO}_2$ ($F_{1,44} < 0.01$, $p = 0.96$, $\eta^2_p < 0.01$), temperature ($F_{1,44} = 0.01$, $p = 0.90$, $\eta^2_p < 0.01$), or the interaction ($F_{1,44} < 0.01$, $p = 0.98$, $\eta^2_p < 0.01$).

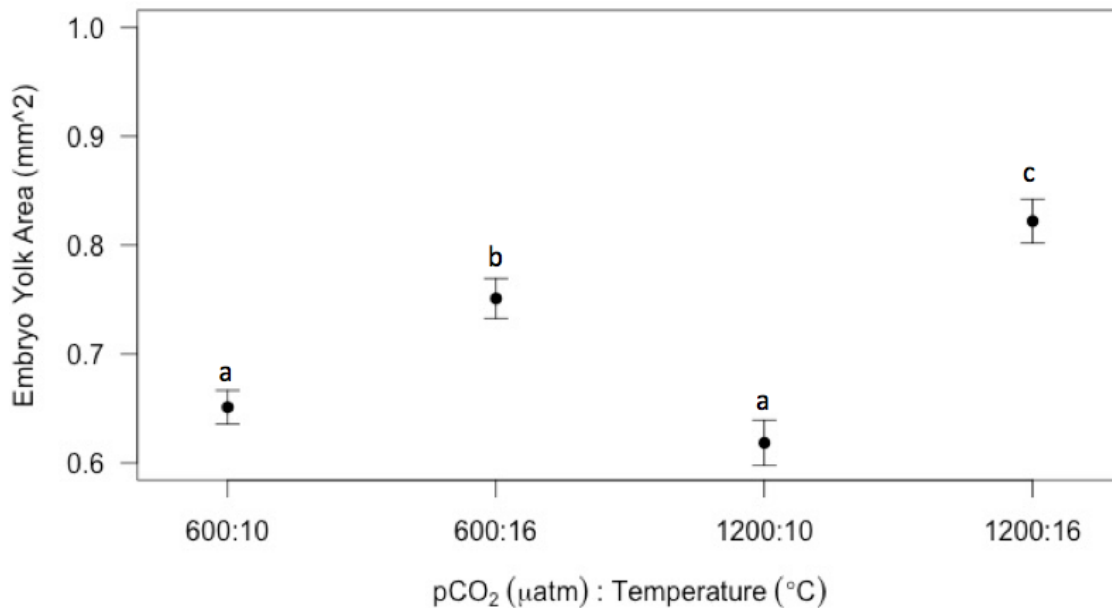


Figure 7: Pacific herring embryo yolk area for each treatment combination. Data are from images collected over two days before the developing embryo obscured the yolk sac (days 9-10 at 10°C, and 3-4 at 16°C). Data are based on the mean \pm 1 SD of (n) measurements: 600:10 (n = 60), 1200:10 (n = 54), 600:16 (n = 49), and 1200:16 (n = 43). Two-way ANOVA analyses indicate yolk area was significantly affected by increased temperature ($F_{1,202} = 62.9$, $p < 0.0$, $\eta^2_p = 2.3$) and the interaction of 1200 $\mu\text{atm} + 16^\circ\text{C}$ ($F_{1,202} = 7.6$, $p = 0.00$, $\eta^2_p = 0.03$).

Table 2: Two-way ANOVA results for average Pacific herring percent normal hatch (% of live non-malformed larvae/initial embryos), abnormal larvae upon hatch (% malformed larvae/initial embryos), and embryo mortality post-fertilization (% of dead embryos/initial embryos). Data are represented by the mean \pm 1 SD of 12 measurements. * Indicates significance.

Percent Normal Hatch	Df	Sum Sq	Mean Sq	F value	Pr(>F)	η^2_p
<i>p</i> CO ₂	1	503.1	503.1	1.96	0.16	0.04
Temperature	1	14145.3	14145.3	55.1	<0.01*	0.55
<i>p</i> CO ₂ :Temperature	1	26.1	26.1	0.10	0.75	0.002
Error	44	11291.7	256.6			
Abnormal Hatch						
<i>p</i> CO ₂	1	255.8	255.7	2.14	0.15	0.04
Temperature	1	85.3	85.3	0.71	0.40	0.01
<i>p</i> CO ₂ :Temperature	1	86.9	86.9	0.72	0.39	0.01
Error	44	5255.1	119.4			
Embryo Mortality						
<i>p</i> CO ₂	1	1297.9	1297.9	4.57	0.03*	0.09
Temperature	1	11322.2	11322.2	39.8	<0.01*	0.47
<i>p</i> CO ₂ :Temperature	1	283.2	283.2	0.99	0.32	0.02
Error	44	12491.7	283.9			

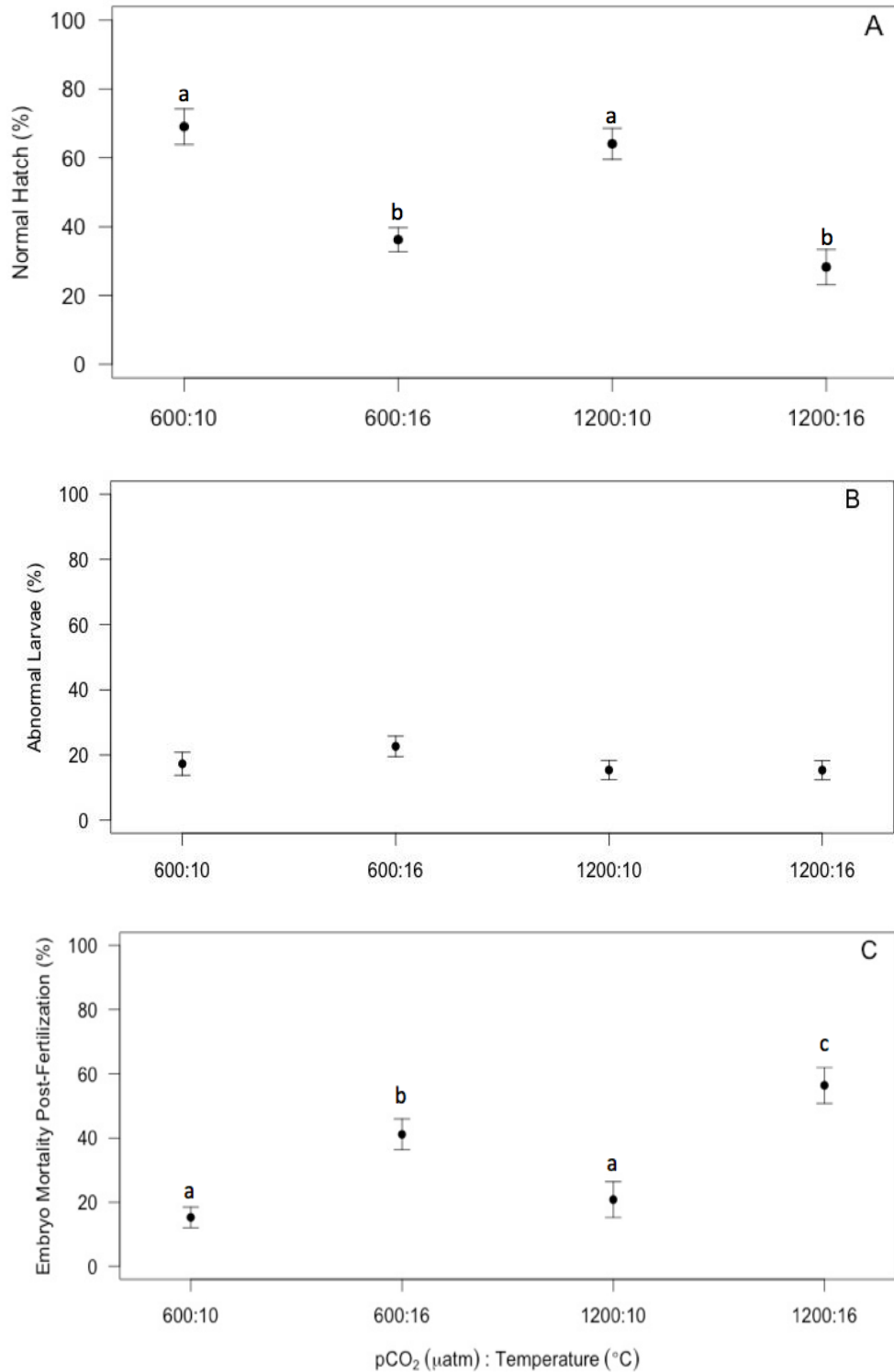


Figure 8: Effects of increased $p\text{CO}_2$ and temperature on Pacific herring normal hatch (A), abnormal larvae (B), and embryo mortality (C). Data represent the mean \pm 1 SD of the percentage per slide, where there were 12 slides in the three basins for each treatment. Lower-case letters indicate statistically different treatments based on a Fisher's LSD post hoc comparison.

Oxygen Consumption

A two-way ANOVA, with temperature and $p\text{CO}_2$ as fixed factors, showed a significant interaction effect on oxygen consumption (Table 4). However, significance may have resulted from the magnitude of corrections for blanks, which varied widely between treatments in magnitude and sign (Table 3). Therefore, oxygen consumption data were re-analyzed without the blank correction. When the blank corrections were removed, neither temperature, $p\text{CO}_2$, nor their interaction significantly affected embryo oxygen consumption (Table 4, Fig. 9). Overall, the oxygen consumption rates were highly variable between and within treatments, rendering the data difficult to interpret, particularly given the difficulty with reliable blank corrections.

Heart rate measurements, another way to estimate oxygen consumption, were not subject to these difficulties. Due to the different embryo developmental stages in the two temperature treatments, data were evaluated separately for 10°C and 16°C , and heart rates were compared at ambient and elevated $p\text{CO}_2$. Heart rates were not statistically different between the two $p\text{CO}_2$ treatments under ambient temperature and averaged 46 bpm overall (Table 5, Fig. 10A). Under the warmer temperature, elevated $p\text{CO}_2$ embryos had a significantly greater heart rate (Table 5, Fig. 10B). Average heart rates increased from 78 bpm at the ambient $p\text{CO}_2$ ($600 \mu\text{atm} + 16^\circ\text{C}$), to 86 bpm at the elevated $p\text{CO}_2$ ($1200 \mu\text{atm} + 16^\circ\text{C}$). This represents a 9% increase in heart rate associated with the elevated $p\text{CO}_2$.

Table 3: Averaged oxygen consumption rates in the blank vials with ± 1 SD of (n) measurements.

Blank Treatment	Blank O_2 consumption rates ($\text{mg/L O}_2 \cdot \text{min}^{-1}$)
$600 \mu\text{atm} + 10^\circ\text{C}$	-5.34 ± 2.86 (3)
$600 \mu\text{atm} + 16^\circ\text{C}$	-0.33 ± 0.02 (2)
$1200 \mu\text{atm} + 10^\circ\text{C}$	2.54 ± 2.71 (3)
$1200 \mu\text{atm} + 16^\circ\text{C}$	-1.31 ± 1.27 (3)

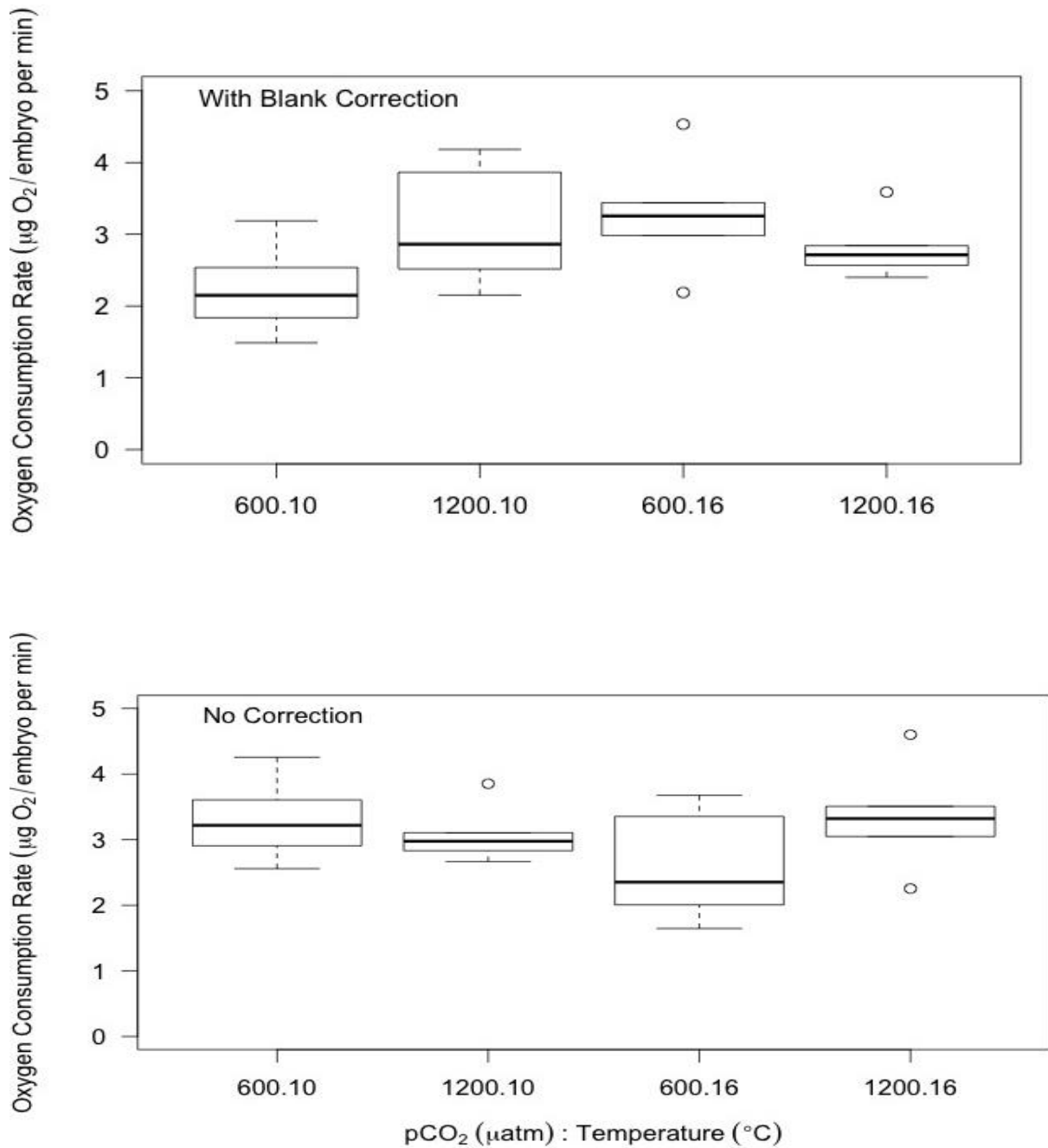


Figure 9: Boxplot depicting embryo oxygen consumption measurements between treatments with and without blank corrections. Each box represents the average rates from six measurements, two vials from each of three basins. Rates are shown as positive values for interpretation.

Table 4: Two-way ANOVA results from the embryo O₂ consumption experiment with and without blank vial corrections. Significance observed in the blank corrected data is likely caused by the variable O₂ consumption rates calculated in the blank vials, and not a treatment effect.

With Blank Corrections	Df	Sum Sq	Mean Sq	F value	Pr(>F)	η^2_p
<i>p</i> CO ₂	1	0.21	0.21	0.48	0.49	0.02
Temperature	1	0.91	0.91	2.08	0.16	0.09
<i>p</i> CO ₂ :Temperature	1	2.61	2.61	5.94	0.02*	0.22
Error	20	8.81	0.44			
Without Blank Corrections						
<i>p</i> CO ₂	1	0.45	0.45	1.03	0.32	0.04
Temperature	1	0.31	0.31	0.70	0.41	0.03
<i>p</i> CO ₂ :Temperature	1	1.51	1.51	3.43	0.07	0.14
Error	20	8.81	0.44			

Table 5: One-way ANOVA results from the embryo heart rate video recordings for both temperature treatments. * Indicates significance.

Ambient Temperature	Df	Sum Sq	Mean Sq	F value	Pr(>F)	η^2_p
<i>p</i> CO ₂	1	39.6	39.6	0.53	0.46	0.00
Error	141	1037	73.5			
High Temperature						
<i>p</i> CO ₂	1	921	921	8.21	0.00*	0.12
Error	60	6729	112			

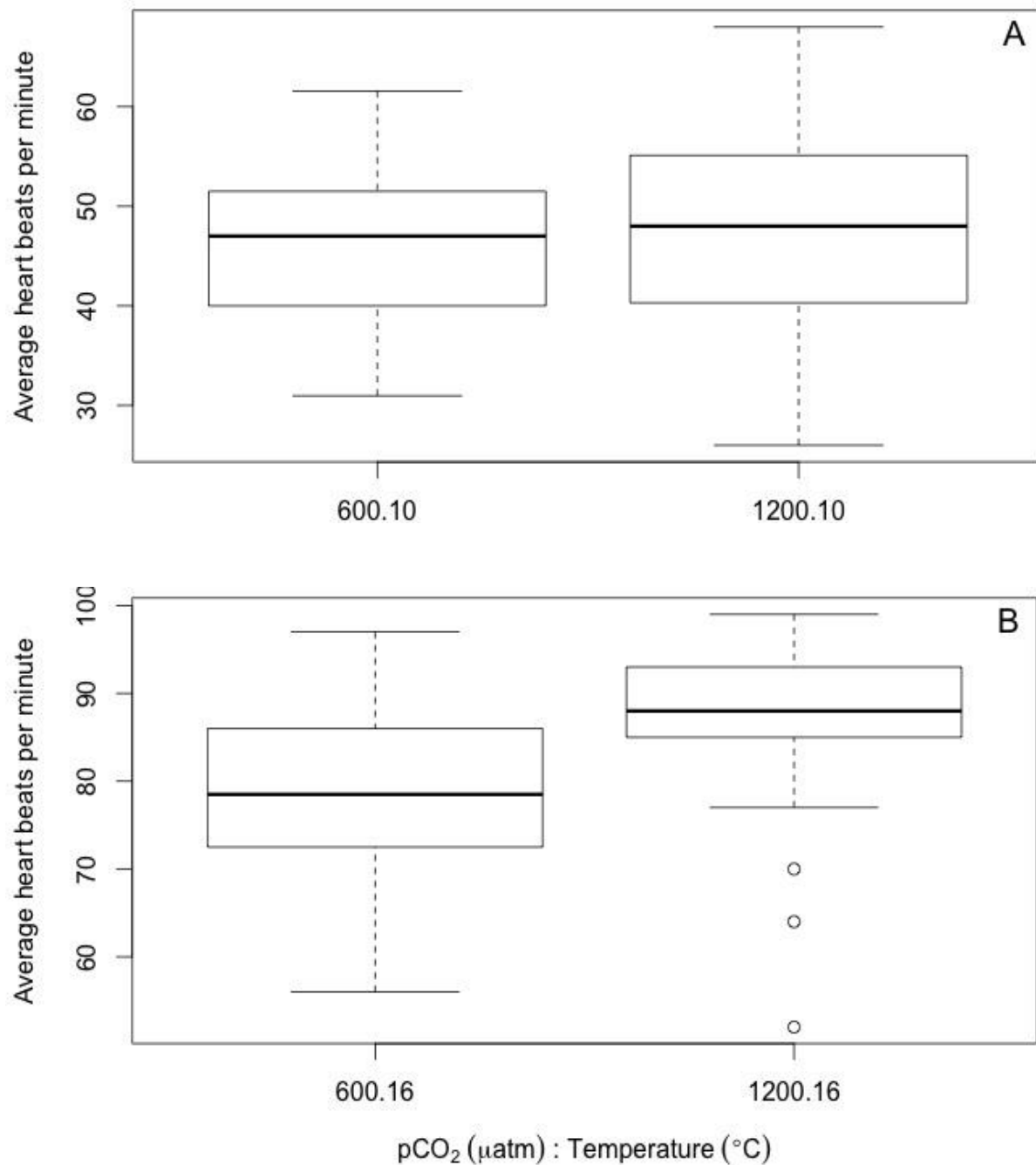


Figure 10: Plots of ambient temperature with $p\text{CO}_2$ (A), and high temperature with $p\text{CO}_2$ (B), on Pacific herring embryo heart rates recorded during one-minute intervals. Recordings occurred on either on day 4 (16°C), or day 5 and 6 (10°C). Data are based on the mean \pm 1 SD of (n) measurements; 600:10 (n = 72), 1200:10 (n = 71), 600:16 (n = 32), and 1200:16 (n = 30).

Larval Morphology

Body lengths of recently hatched larvae were significantly affected by temperature ($F_{1,41} = 75.5, p < 0.01, \eta^2_p = 0.34$), but not by $p\text{CO}_2$ ($F_{1,141} = 0.0, p > 0.05, \eta^2_p = 0.00$). Larvae reared at low temperature (600 $\mu\text{atm} + 10^\circ\text{C}$) had an average length of 6.4 mm, compared to an average length of 5.6 mm for larvae reared at the high temperature (600 $\mu\text{atm} + 16^\circ\text{C}$), indicating a 12% shorter length with increasing temperature (Fig. 11A). Lengths were also shorter by an average of 16% between the low and high temperature treatments at high $p\text{CO}_2$ (1200 $\mu\text{atm} + 10^\circ\text{C}$ to 1200 $\mu\text{atm} + 16^\circ\text{C}$), indicating that the magnitude of the temperature effect did not change with $p\text{CO}_2$ treatment. This relationship is further supported by the lack of a significant interaction effect of temperature and $p\text{CO}_2$ ($F_{1,141} = 1.1, p > 0.05, \eta^2_p = 0.00$). Larval lengths were also significantly affected by temperature as a function of hatch date (Fig. 12, Table 6). Within the ambient temperature, day's post-fertilization was a stronger indicator for larval size upon hatch ($R^2 = 0.82$, Fig. 12), than in the warmer temperature treatment ($R^2 = 0.37$, Fig. 12).

Average dry weights did not significantly differ among treatments, averaging 0.08 mg per larvae ($p > 0.05$) (Fig. 11B). Larval dry weights were further examined by comparing weights at both temperatures during the maximum hatch date (14 days post-fertilization at 10°C ; 9 days post-fertilization at 16°C). Dry weights during max hatch appeared to be greater in the warmer temperature treatment (Fig. 13), however the differences were not statistically different ($F_{1,26} = 2.2, p > 0.05, \eta^2_p = 0.08$).

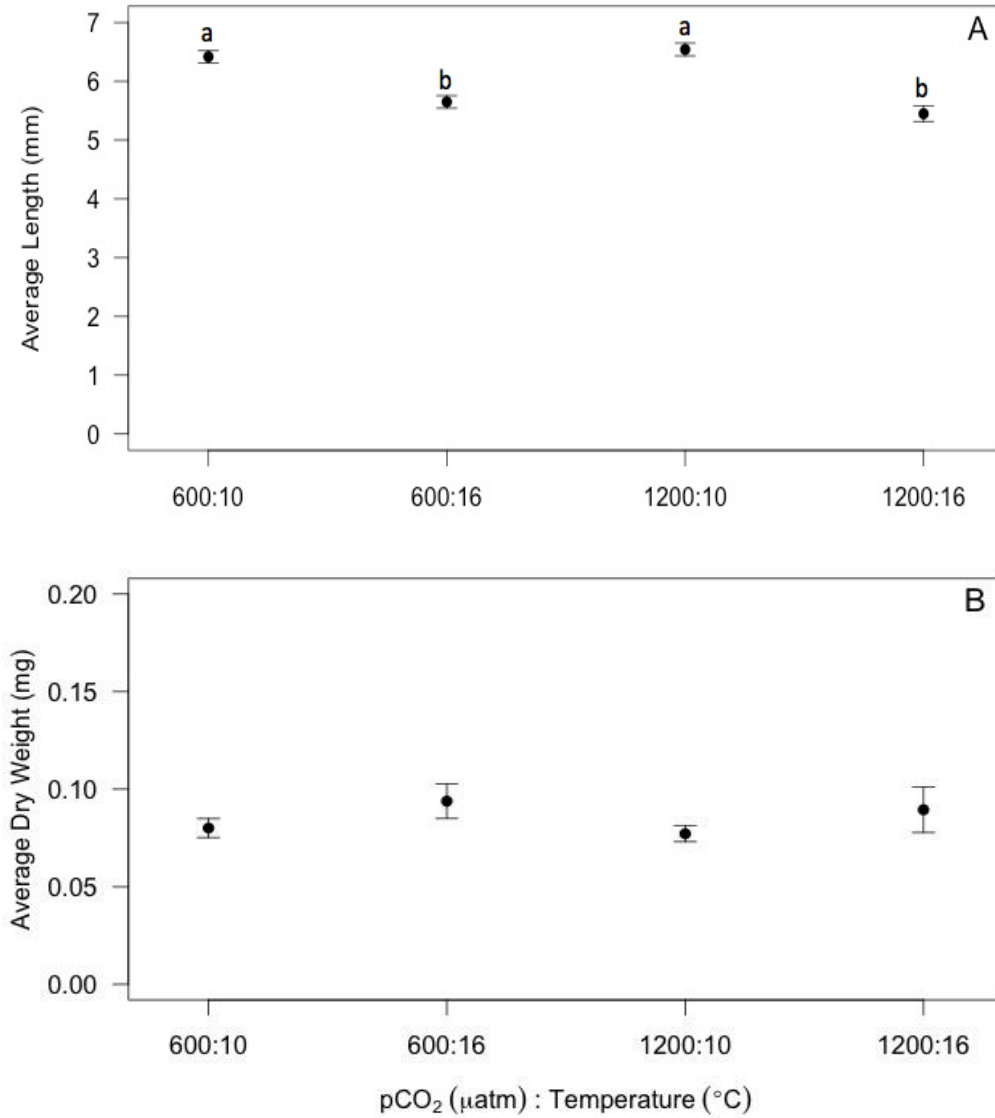


Figure 11: Effects of increased $p\text{CO}_2$ and temperature on the average length (A) and dry weight (B) of Pacific herring larvae. Length data are represented by the mean \pm 1 SD (n) of larvae measurements for 600:12 (n = 414), 600:16 (n = 338), 1200:10 (n = 425), and 1200:16 (n = 271). Weight data are represented by the mean \pm 1 SD (n) of larvae measurements for 600:12 (n = 313), 600:16 (n = 240), 1200:10 (n = 302), and 1200:16 (n = 181). Lower-case letters indicate statistically different treatments based on a Fisher's LSD post hoc comparison.

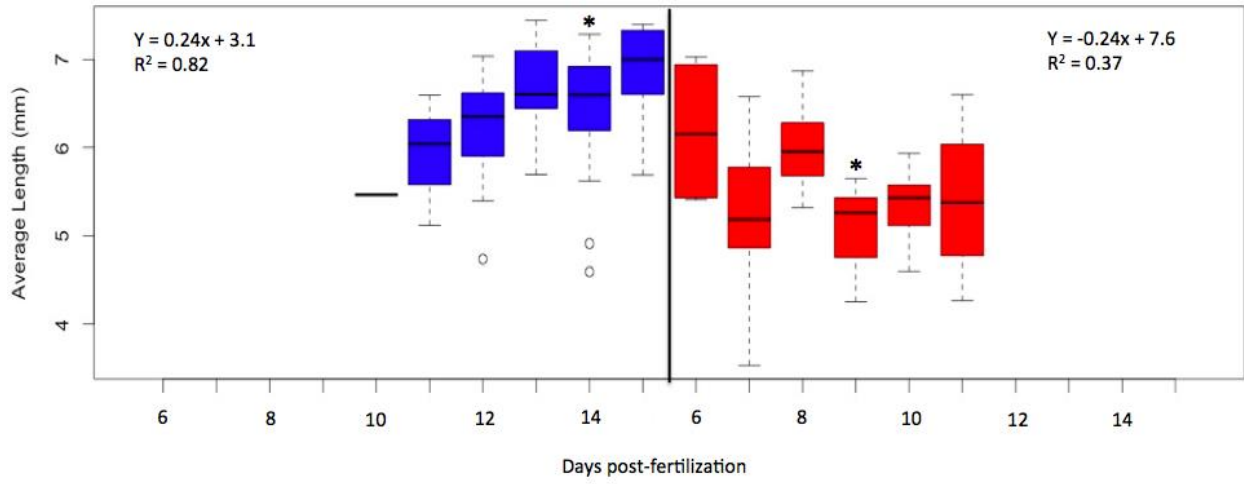


Figure 12: Average Pacific herring larvae lengths (mm) upon hatch as a function of hatch date and temperature treatment; with $p\text{CO}_2$ pooled within temperature. Blue colored boxplots (10°C treatment) and red colored boxplots (16°C treatment) are separated by the black vertical line, which signifies the time axis for 16°C . The black asterisk indicates the date with the maximum number of live, hatched larvae for both temperature treatments. Regression statistics in the upper plot corners are based on the averaged larval length values for each day.

Table 6: Two-way ANOVA results for larvae lengths (mm) as a function of hatch date and temperature treatment. * Indicates significance

Factor	Df	Sum Sq	Mean Sq	F value	Pr(>F)	η^2_p
Date	1	29.6	29.6	69.4	<0.01*	0.32
Temperature	1	3.19	3.19	7.47	<0.01*	0.05
Date:Temperature	1	1.71	1.71	4.02	0.04*	0.02
Error	141	60.1	0.42			

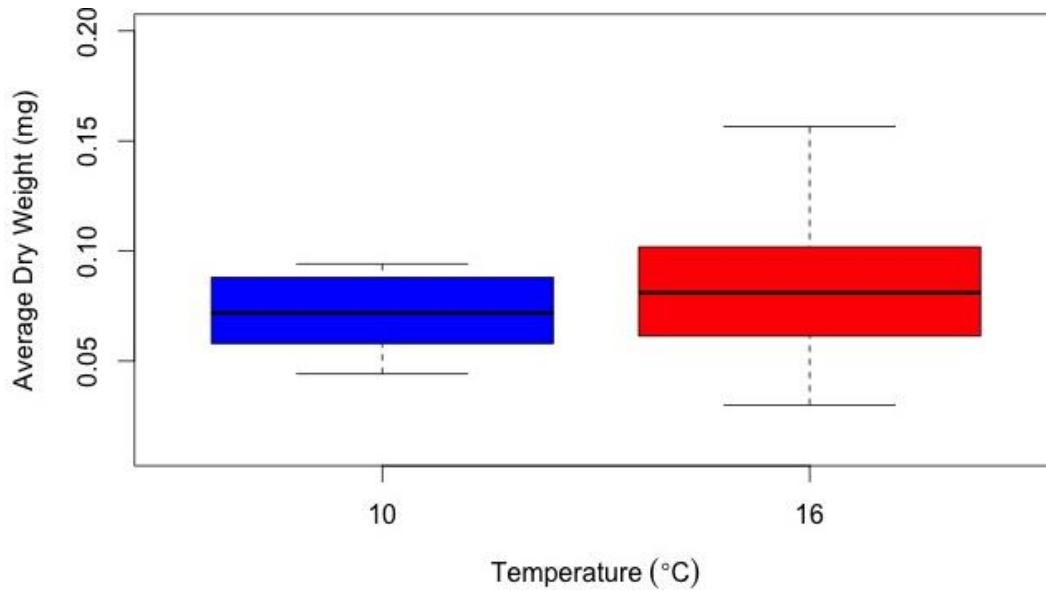


Figure 13: Average Pacific herring larvae dry weights from the max hatch date for both temperature treatments. Data represent values from weigh boats containing 10 or more larvae. Differences between average dry weights were not statistically different ($F_{1,26} = 2.2$, $p > 0.05$, $\eta^2_p = 0.08$).

Discussion

Effects of pCO_2

Pacific herring embryos appear largely unaffected by pCO_2 levels up to 1200 μatm . Elevated pCO_2 , as a single stressor, did not impair Pacific herring fertilization, percent normal hatch, embryo heart rates, or larval morphology. These findings indicate embryos and larvae upon hatch may be robust to 600-1200 μatm of pCO_2 , however, elevated pCO_2 was associated with an increase in embryo mortality. Pacific herring embryos may already be periodically or episodically exposed to near future acidification levels during development and may be accustomed to fluctuating CO_2 levels. Herring embryos may have developed genetic adaptation and phenotypic plasticity resulting from the natural pCO_2 variability in their habitat.

For example, while present mean surface ocean pCO_2 values average around 400 μatm , greater values occur in intertidal regions, estuaries, and upwelling coastal zones (Wotton et al.,

2008; Feely et al., 2008, 2010; Melzner et al., 2009). Along the eastern boundary current of North America, elevated $p\text{CO}_2$ values nearing 1000 μatm have been documented off the Californian coast (Feely et al., 2008). Upwelled water, and estuarine circulation is another mechanism for high $p\text{CO}_2$ intrusion along the outer Washington coast, where Feely et al. (2010) documented pH values of 7.71 to 8.05 within the Juan de Fuca Canyon and Juan de Fuca Strait.

Estuaries and intertidal regions experience short-term fluctuations in $p\text{CO}_2$ due to photosynthetic and respiration activity, where $p\text{CO}_2$ values can approach 3500 μatm (Truchot and Duhamel-Jouve, 1980). In Puget Sound, nutrients from terrestrial runoff can trigger high organic matter production that is ultimately respired to CO_2 (Feely et al., 2010). The average daily pH can range from 7.7 to 8.4 in the Padilla Bay estuary (Baumann and Smith 2018). Time series water quality data (September 2011 to July 2013) from Friday Harbor Laboratories dock (~ 3 m depth) showed consistent average $p\text{CO}_2$ concentrations of ~ 650 μatm (pH 7.8) (Murray et al., 2015), which was the average ambient pH during Pacific herring embryo incubation. Surface $p\text{CO}_2$ /pH seawater away from shore, east of the San Juan Islands, show similar conditions during the fall of 2011 ($p\text{CO}_2 \sim 711\text{--}1081$; pH 7.67–7.80) (Sullivan 2013).

Ocean acidification research on other North Pacific fish species indicates resiliency parallel to Pacific herring early life stages. For example, Hurst et al. (2014) reared Northern rock sole (*Lepidopsetta polyxystra*) early life stages under a range of experimental CO_2 values (reaching up to 1500 μatm). They found no significant effects of CO_2 on embryo survival or larval growth. Northern rock sole inhabit regions within the Gulf of Alaska where adults spawn in shallow water. Larvae settle into inner coastal areas where they are more likely subjected to periodic CO_2 fluctuations (Hurst et al., 2014).

Walleye pollock (*Theragra chalcogramma*) larvae seize metrics were not affected at

$p\text{CO}_2$ levels up to 2000 μatm (Hurst et al., 2013). Walleye pollock also reside in the Gulf of Alaska but have differing life history traits than the Northern rock sole. Walleye pollock spawn at depths of 50 m and larvae drift at depths down to 200 m in the Gulf of Alaska (Hurst et al., 2013). These midwater pelagic areas experience less short-term variation in CO_2 levels than shallow coastal waters (Hofmann et al., 2011; Busch, 2012), and pollock may be adapted to this relatively stable CO_2 environment, suggesting a possibly greater sensitivity to changes in $p\text{CO}_2$.

For experiments, Hurst et al. (2013) used offspring from a laboratory-maintained broodstock of fish caught from Puget Sound, WA where some areas currently experience pH levels below 7.7 (Feely et al., 2010). Walleye pollock embryos from a Puget Sound population may have preconditioned to high CO_2 levels, and the embryos were therefore resilient to the elevated $p\text{CO}_2$ conditions (Hurst et al., 2013). The effects of $p\text{CO}_2$ on different fish species show high response variability, and evidence suggests the disparity may be related to the local variability in $p\text{CO}_2$ dynamics.

While it is difficult to compare ocean acidification responses across different species, investigating the responses of related fish species within a single study allows a closer comparison. Along the California current ecosystem, the life history of two congener rockfish species, the blue rockfish (*Sebastes mystinus*) and copper rockfish (*S. caurinus*) appears to have shaped their tolerance to elevated $p\text{CO}_2$ (Hamilton et al., 2017). Both rockfish species reside in kelp forests along the U.S. West Coast, and although these two congener species are closely related evolutionarily, they differ by spatial distribution within kelp forests and timing of spawn (Lenarz et al., 1991). Copper rockfish spawn in spring and for several months larvae develop close to the surface, with juveniles settling near the kelp canopy where $p\text{CO}_2$ is locally variable due to kelp photosynthesis and respiration (Hamilton et al., 2017).

Blue rockfish spawn in winter and larvae develop deeper in the water column. Blue rockfish juveniles settle near the benthos where $p\text{CO}_2$ is locally elevated due to respiration and upwelling plumes (Hamilton et al., 2017). Thus, blue rockfish larvae are likely better adapted to future, elevated $p\text{CO}_2$ conditions than copper rockfish larvae. When juvenile stages of both rockfish species were chronically reared in elevated $p\text{CO}_2$ (~2800 μatm), copper rockfish showed greater impairment in neurological functions, swimming speed, and aerobic scope compared to blue rockfish, which showed no significant changes (Hamilton et al., 2017). These species-specific differences in physiological tolerances to $p\text{CO}_2$ exposure may be explained by genetic adaption, from long-term exposure of the population, or acclimatization from individual responses during experimentation (Hamilton et al., 2017).

While studies on $p\text{CO}_2$ effects have not been conducted on Pacific herring, there are several studies on Atlantic herring, a closely related species. Atlantic herring embryogenesis was found to be resilient to $p\text{CO}_2$ levels up to 4300 μatm (Franke and Clemmesen 2011). However, in the larval stages of Atlantic herring, larvae somatic growth is reduced under elevated $p\text{CO}_2$ (> 1800 μatm) compared to the larvae from control $p\text{CO}_2$ levels (~ 370 – 400 μatm) (Maneja et al., 2014; Frommel et al., 2014). Larval survival was also significantly reduced under $p\text{CO}_2$ concentrations of 900 μatm compared to 400 μatm (Sswat et al., 2018a). However, the negative $p\text{CO}_2$ effects on Atlantic herring larvae may be countered by the presence of an abundant food supply (Sswat et al., 2018b). In a recent study using Atlantic herring embryos incubated under two $p\text{CO}_2$ (~380 and 760 μatm), the hatched larvae were fed similar prey abundances found in their natural nursery areas (Sswat et al., 2018b). The results showed that the larvae experienced significantly greater survival under the high $p\text{CO}_2$ (3.2%) compared with the control (1.2%), indicating the high $p\text{CO}_2$ conditions improved the food supply for herring larvae and contributed

to greater survival.

Hypercapnia in the embryo membrane may be normal part of development, however, high environmental CO₂ can increase, and potentially contribute to, embryo mortality. In this study, Pacific herring embryo mortality increased by 7% from the ambient to the elevated *p*CO₂ when at ambient temperature (10°C). During embryo gestation, the egg case may slow CO₂ and O₂ diffusion, creating hypercapnic and hypoxic conditions within the membrane as the embryo develops (Melzner et al., 2009). This occurred within the cephalopod's, *Sepia officinalis*, egg casing (~2 cm diameter) where *p*CO₂ increased from 1300 to 4000 µatm for several weeks during development (Gutowska and Melzner, 2009). This finding indicates that hypercapnia is a regular part of the life cycle of *S. officinalis* and hypercapnia may also exist as a natural influence for Pacific herring during ontogeny.

However, Pacific herring embryos are smaller in diameter (~1.5 mm: Lassuy 1989), increasing the surface area to volume ratio and allowing a more effective rate of CO₂ diffusion across the egg casing than *S. officinalis*. The diffusion rate depends on the gradient across the membrane, and if external *p*CO₂ is high, then diffusion may slow, resulting in more elevated internal *p*CO₂. Because there was no difference in embryo size across treatments (Appendix A, Fig. A2), the surface area to volume aspect on the *p*CO₂ effects on embryo development was not relevant in this study. The decreased diffusion rate given higher external *p*CO₂ is one potential factor in the increased heart rates observed in the high temperature, high CO₂ embryos. Greater CO₂ concentrations within a teleost's bloodstream hinder the ability of oxygen to effectively bind to oxygen transporting cells (Bohr effect). Therefore, when external *p*CO₂ is high, diffusion out of the bloodstream is low, internal *p*CO₂ is increased, and oxygen binding is decreased. Increased heart rates in Pacific herring embryos, within the warmer temperature and interaction

treatment, may have been an adaptive mechanism to obtain more oxygen from their environment and overcome the limitations of oxygen solubility (associated with increased temperature), and limited oxygen binding capacity (associated with increased $p\text{CO}_2$).

Adult Pacific herring primarily deposit embryos on marine vegetation, such as eelgrasses (Lassuy 1989). Seagrasses potentially buffer the effects of ocean acidification by removing dissolved inorganic carbon (DIC) from seawater during photosynthesis, and lowering $p\text{CO}_2$ levels within the surrounding environment (Beer and Rehnberg 1997; Unsworth et al., 2012). Miller et al. (2017) measured CO_2 uptake by both native (*Zostera marina*) and non-native (*Zostera japonica*) species of eelgrass from Padilla Bay, WA. Both species showed rates that were sufficient to alter local seawater carbonate chemistry, depending on water depth, light conditions, shoot density, epiphyte communities, tidal change, and other factors affecting carbonate chemistry. Eelgrass carbon uptake rates may not fully lessen the severity of episodic acidification, but future work can focus rearing Pacific herring embryos on eelgrass and under a range of $p\text{CO}_2$ conditions. This will more precisely determine how Pacific herring early life stages will be affected by acidification in its environment – including localized $p\text{CO}_2$ decreases, and increased variability in carbonate chemistry conditions from dense marine vegetated areas (Pacell et al., 2018).

Effects of Temperature

Across a range of marine organisms, temperature is a key factor in determining developmental time (Harley et al., 2006; Doney et al., 2012). The warmer temperature treatment contributed to the significant differences found in Pacific herring embryo mortality, heart rates, percent normal hatch, and larval lengths in this study. Warmer temperatures can affect embryo

survival by two mechanisms. First, as seawater temperatures rise, dissolved oxygen decreases due to decreased solubility, resulting in lower oxygen availability. Some marine embryos depend on diffusion to supply oxygen for metabolism. For Nudibranch embryos, when metabolic rates are high, diffusion can become an insufficient process for delivering enough oxygen to meet the embryos demand (Moran and Woods 2010). Second, thermal windows can be narrow in fish embryos, and as temperatures rise, the demand for oxygen becomes greater while the available supply may be diminishing (Rombough 1997; Pörtner 2001; Pörtner 2012). For example, Dahlke et al. (2016) showed that for Atlantic cod, whole-embryo oxygen consumption rates increased by an average change of 11% over the 0 to 9°C temperature range.

Pacific herring embryos exhibited a 14% increase in heart rates from the ambient to high temperature treatments (600 $\mu\text{atm} \pm 10^\circ\text{C}$ to 600 $\mu\text{atm} \pm 16^\circ$). Because the embryos were at different developmental stages in the two treatments when this measurement was taken, this comparison should be interpreted cautiously. However, this potential increase in embryo heart rates could suggest an oxygen deficit within the basins at the warmer temperature, and may be linked to Pacific herring embryo mortality. Warmer temperatures contribute to a mismatch between oxygen solubility, embryo oxygen demand, and the ability for embryos to take up oxygen.

Greater oxygen demands under warmer temperatures may be the determining factor affecting Pacific herring embryo survival and possibly compromising larval morphology. Increased Pacific herring embryo heart rates may also reflect an attempt to meet a greater energy demand, as its development is accelerated under warmer temperatures. Our oxygen consumption data were difficult to interpret because of the high variability and cannot be used to confirm the suggestion of higher metabolic rates under the warmer temperature in this study.

Q_{10} , a measure of how a ten degree temperature change influences a system, varies from about 1.5-4.9 for metabolic rates in marine fish species (Peck and Moyano 2016). Although Pacific herring Q_{10} values have yet to be evaluated, the Q_{10} for Atlantic herring larvae oxygen consumption is reported as 1.5 (Peck and Moyano 2016). Given this Q_{10} , an increase in oxygen consumption rate of 27% would be predicted for the 6°C difference in this study. Our oxygen consumption data for Pacific herring embryos were variable, however this predicted Q_{10} may fall within the range of our measurements. Our oxygen consumption data do not show a strong effect of temperature, however, the variability within each treatment is much higher than this expected effect and may have obscured detection. Our heart rate, data however can provide another measure of metabolic rate.

Heart rate patterns vary in teleost species during development, but heart rate Q_{10} values are typically greater during larval life stages (Mirkovic and Rombough 1997; Barrionuevo and Burggren 1999; Peck and Buckley 2008). Previous research on Atlantic cod, *Gadus morhua*, indicate that temperature had a greater influence on larvae than in juveniles, with respiration rate Q_{10} values decreasing with increasing dry body mass (Fig. 2, Peck and Buckley 2008). The Q_{10} for heart rate also varies depending on temperature, with lower Q_{10} values at greater temperatures. For the zebrafish, *Danio rerio*, heart rate Q_{10} values were ~2 at the embryo stage, peaked at ~2.5 on day 40 under the 25-28°C treatment, and then decreased with development (Barrionuevo and Burggren 1999). When measured closer to the upper end of the temperature range (28-31°C), zebrafish Q_{10} values were below 2 as an embryo, peaked at ~2 on day 60, and decreased to ~1.5 on day 100.

Based on our Pacific herring embryo heart rate data, a 6°C difference yields a Q_{10} of 1.4. This Q_{10} value for Pacific herring embryo heart rate is similar to the Q_{10} value of 1.5 for oxygen

consumption in Atlantic Herring. It is necessary however to determine how closely the Q_{10} values would be expected to match for these two different measures. Rainbow trout, *Oncorhynchus mykiss*, larvae show a similar pattern with heart rate $Q_{10} \sim 3.06$ similar to oxygen consumption $Q_{10} \sim 2.99$ (Mirkovic and Rombough 1997). Therefore, it seems that the metabolic response of Pacific herring to temperature change is similar to that of Atlantic Herring, however tests were not done at the same temperature range or developmental stage. Furthermore, differences in heart rate and oxygen consumption Q_{10} values change as teleost species mature and their primary method of obtaining oxygen evolves from diffusive gas exchange to more developed respiratory structures, such as gills. Heart rate and oxygen consumption then become more tightly coupled as teleost larvae develop (Fig. 6, Mirkovic and Rombough 1997).

Overall, our calculated Q_{10} of 1.4 for Pacific herring is on the lower end for the average Q_{10} values reported by Peck and Moyano (2016). This could indicate that this species is less sensitive to increases in temperature than others which may be adapted for more stable temperature conditions, whereas the nearshore and coastal habitats of Pacific herring do experience natural variability in temperature. However, this low value may also be partially due to testing conditions. Pacific herring oxygen consumption and heart rate data were recorded during the embryo stage when the Q_{10} is typically lower, and may increase at the larval stage. Additionally, an upper temperature of 16°C may have been near the upper range for Pacific herring development and further contributed to a lower Q_{10} . Establishing this Q_{10} baseline for Pacific herring will provide an additional resource for understanding environmental constraints on their early growth and survival.

Under warmer temperatures, Atlantic cod cumulative embryo survival progressively decreased (63% at 6°C, 42% at 9°C, and 25% at 12°C), suggesting embryo survival was

dependent on its capacity to meet the above-mentioned oxygen and energy demand (Dahlke et al., 2016). Our study showed that embryo mortality increased by an average of 26% from the low to high temperature treatments at ambient $p\text{CO}_2$ ($600 \mu\text{atm} \pm 10^\circ\text{C}$ to $600 \mu\text{atm} \pm 16^\circ\text{C}$), and percent normal hatch decreased significantly by 29% from 10°C to 16°C , regardless of $p\text{CO}_2$.

Pacific herring larvae post-hatch were significantly shorter in length when reared at 16°C (Fig. 10A, Fig. 11). A change in energy demand at the embryo stage potentially allocates energy away from other developmental processes, such as muscle development (Baumann et al., 2011). Differences in larval lengths between the two temperature treatments may be attributed to embryo incubation time. In the present study, Pacific herring embryos began hatching five days sooner in the 16°C treatment than at 10°C (Appendix A, Fig. A1). Embryo development is assumed to continue throughout the entire incubation period and that hatching is an age-related event (Geffen 2002). Geffen (2002) showed that later hatching Atlantic herring larvae were longer because they continued to grow within the embryo membrane. This study did not initially detect differences in embryo diameters, which may indicate larval size upon hatch, across treatments (Appendix A, Fig. A2).

Under warmer temperatures, reduced larval size at hatch for Atlantic cod was associated with greater energy demands and higher oxygen consumption rates (Dahlke et al. 2016). Overall, it is possible that Pacific herring larvae that hatched sooner at 16°C were shorter in length due to a shortened incubation period, and that energy is being allocated differently to meet a greater energy demand, leaving less energy available for growth. It may also be an adaptive response under warmer temperatures to hatch sooner. For example, faster growing embryos would experience greater O_2 demand, and growth may not be favored if O_2 is limited, due to the warmer temperature reducing O_2 solubility. Therefore, larvae may emerge from the embryo

casing sooner to remove the diffusion barrier.

Larval dry weights did not statistically differ between treatments or during the maximum hatching period between both temperatures: an examination of larvae yolk sacs in prematurely hatched larvae may provide an explanation. Yolk conversion efficiency reaches a maximum within the thermal tolerance range of a given species and tends to decrease near the upper and lower boundaries of tolerated temperatures (Galloway et al., 1998). For example, Atlantic cod embryos incubated at a low temperature (1°C) produced smaller larvae with larger yolk sacs, than embryos incubated at 5 or 8°C (Galloway et al. 1998). They suggest that the reduced larval size obtained at the low temperatures may be a sub-lethal response to an unfavorable environment.

On the other hand, under increased temperature (12°C) and $p\text{CO}_2$ (1100 μatm), Atlantic cod embryo energy demand was shown through higher metabolic rates and reduced larval size at hatch, while the consumption of yolk reserves remained unaffected, indicating embryos were not able to convert yolk energy to other physiological functions (Dahlke et al., 2016). In this study, Pacific herring larvae reared within the 1200 μatm +16°C treatment had the largest yolk area. Greater yolk areas indicate less yolk was used for other developmental processes, such as growth. This may explain why no differences were detected in larval dry weights, because mass either remained within the yolk sac for larvae that hatched sooner under the warmer temperature treatment or was converted into growth for larvae in the ambient temperature treatment.

Although warmer rearing temperatures lead to faster Pacific herring embryo development, an earlier hatch time is not necessarily advantageous. Accelerated growth can also lead to abnormal muscle development, which may increase the probability of larvae hatching with jaw, spinal, or pectoral malformations – hindering a larvae's ability to avoid predators and

capture prey (Vieira and Johnston 1992; Green and Fisher 2004). Shorter larval lengths at hatch may have an indirect effect on swimming performance. For example, shorter lengths (~ 7 mm total length difference) decreased swimming velocity (m s^{-1}) by 24% of Atlantic herring larvae (Johnston et al. 2001). Sswat et al. (2018a) found significantly greater swimming activity in the longer Atlantic herring larvae with increasing temperature (12°C), compared to shorter larvae from the lower temperature (10°C).

Under the ‘bigger is better’ hypothesis shorter larvae would be at a disadvantage, in that bigger larvae are more likely to survive given its ability to outcompete smaller and slower larvae (Green and Fisher 2004). Reduced swimming velocity may also alter larvae distribution in the water column and affect the survival of juvenile and adult life stages by failing to settle in preferred habitats (Johnston et al. 1998). This study did not measure the swimming or feeding performance of Pacific herring larvae, but the percentages of abnormally hatched Pacific herring larvae were not significantly different between treatments.

In Pacific herring early life stages, increased temperature was the primary driver affecting embryo and larval responses. These observations occurred at an experimental temperature of 16°C . In the Puget Sound, the average temperature vary 6.6°C to 16.4°C in nearshore areas depending on the season (Baumann and Smith 2018). During early spring Pacific herring spawn months, seawater temperatures are near 9 to 13°C , depending on depth (WDFW herring trawl surveys). Our experimental temperature of 16°C was above the typical spawning temperature that Pacific herring experience stressing the embryos and contributing to greater embryo mortality, oxygen demand, lower percent normal hatch, and shorter larval lengths.

Organisms have evolved to function efficiently under specific habitat temperatures (Hofmann and Todgham 2010; Doney et al., 2012). When environmental temperatures begin

approaching an organism's thermal limit, survival will depend on the capacity of organisms to maintain physiological processes under thermal stress (Hofmann and Todgham 2010). In response to warming, Pacific herring embryos may have spent more energy on oxygen processes and less energy towards growth. Changes in energetic demands may diminish the ability of Pacific herring early life stages to cope with other interacting, and challenging, conditions found in its environment.

Effects of $p\text{CO}_2$ and Temperature

While Pacific herring inhabit coastal regions with variable $p\text{CO}_2$ and may be adapted to acidification, warming temperatures may exacerbate the effects of $p\text{CO}_2$. Ocean warming appears to increase total energy expenditure for metabolism (Sswat et al., 2018a). Effects on embryonic herring metrics were primarily temperature driven in this study, as seen by the temperature responses in percent normal hatch embryo mortality, heart rates, and larval lengths. Where direct effects of $p\text{CO}_2$ were observed, they were small compared to the temperature effects (i.e. embryo mortality). We observed a significant increase of Pacific herring embryo heart rates, by an average of 9% between 600 μatm +16°C to 1200 μatm +16°C. The effect of $p\text{CO}_2$ on embryo heart rate was only observed under temperature stress (Table 5). The $p\text{CO}_2$ levels at ambient temperature had no effect on heart rates. Interacting stressors also affected embryo yolk area, with more area present in the 1200 μatm +16°C treatment.

This finding demonstrates how the effect of temperature can increase the susceptibility of Pacific herring embryos to high $p\text{CO}_2$. Heart rates and yolk area were significantly affected by the 1200 μatm +16°C treatment in this study, which demonstrates the importance of testing

multiple stressors concurrently. Studies investigating single stressors effects of $p\text{CO}_2$ and warming may miss detecting significant interaction effects.

Other studies investigating multiple stressor effects on teleost embryos have detected significant findings on percent normal hatch and oxygen consumption. Elevated $p\text{CO}_2$ caused a significant decrease in hatching success of Atlantic cod larvae with temperature changes (47% at 0°C, 11% at 9°C, and 42% at 12°C) (Dahlke et al., 2016). In the temperature range of 0 to 9°C, embryo oxygen consumption overall increased by 11% under elevated $p\text{CO}_2$ (1100 μatm) (Dahlke et al., 2016). Di Santo (2014) investigated how interactions of $p\text{CO}_2$ (~ 400 and 1100 μatm) and temperature (15, 18, or 20°C) affected little skate (*Leucoraja erinacea*) embryos. They found increased embryo oxygen consumption under the interaction of high $p\text{CO}_2$ and high temperature combination for a Georges Bank population of little skate. As thermal tolerance windows are related to oxygen supply and energy demand (Pörtner and Knust 2007), the added stress of elevated $p\text{CO}_2$ may further constrain thermal windows and affect the survival of fish early life stages. The greater heart rates in Pacific herring embryos may have been a glimpse into the beginning threshold of thermal tolerance brought on by elevated $p\text{CO}_2$.

Conclusion

Surface seawater temperatures in the PNW are expected to increase 1.9 to 5.2°C by 2041-2070 (Dalton et al., 2013), which will raise the current temperature for Pacific herring spawning in Cherry Point, WA, from 9-13°C to 11-18°C (surpassing the high temperature treatment in this experiment in some cases). Elevated temperature was the primary stressor that increased embryo mortality, reduced normal hatch, contributed to shorter larval lengths, and increased embryo

heart rates in this study. Therefore, the temperatures predicted in PNW waters could have profound effects on herring embryos and populations.

These effects of increasing temperature will be compounded with increasing $p\text{CO}_2$. Our results showed that Pacific herring fertilization success, embryo heart rates, normal hatch, and larval morphology are robust to $p\text{CO}_2$ levels between 600 - 1200 μatm as a single stressor. Therefore, Pacific herring embryo development is not expected to be significantly impaired under current $p\text{CO}_2$ conditions in the Pacific Northwest (PNW). However, the interaction of elevated temperature (16°C) and $p\text{CO}_2$ (1200 μatm) conditions further increased embryo heart rates by 9%, and embryo mortality increased by 15%, from the ambient to high $p\text{CO}_2$ treatments at high temperature (600 $\mu\text{atm} \pm 16^\circ\text{C}$ to 1200 $\mu\text{atm} \pm 16^\circ\text{C}$). Increased heart rates signify potential changes in developmental and metabolic processes that may ultimately hinder Pacific herring early life stages growth and survival. Both environmental changes will occur simultaneously and the above-mentioned negative effects on Pacific herring early life stages will likely be more common.

Our study provides the beginning groundwork for understanding direct ocean acidification and warming effects, but further research into how different food levels (indirect effects) affect marine fish larvae during early life stages are needed. Limited energy uptake due to low prey availability, combined with an increased energy demand, may result in less energy available for growth (Sswat et al., 2018b). However, future conditions could alter for planktonic food webs and supply high food quantity and quality. Examining how food abundance may counteract negative effects in developing Pacific herring larvae will provide further insight into consequences on adult populations. Further research into a broader scope of conditions and multi-generational studies are needed to investigate how this species will respond to varying

environmental stressors over time. Given that Pacific herring spawn among eelgrass in the PNW, understanding how eelgrass may mitigate the effects of ocean acidification will be another critical area of research in determining Pacific herring embryo and larval sensitivity.

Pacific herring are a critical fish species in the Salish Sea ecosystem, with distinct connections throughout the food web. In the Salish Sea, herring are an important prey item sea birds, salmon, and marine mammals (Stick and Lindquist 2009). Pacific herring are not only ecologically important, but they are also a culturally significant species for native Tribes and First Nations in the region (Lassuy et al., 1989). At present, no specific strategies exist for managing the recovery of Puget Sound Pacific herring (Francis and Lowry 2017). Results from this study can aid the Recovery and Assessment Team, which is comprised of representatives from herring management agencies from Washington and BC, university affiliates, First Nations, and Tribes. These research findings will provide an additional source to identify actions, and uncertainties, in order to advance herring conservation and recovery.

References

- Alderdice, D.F., and F.P.J. Velsen. 1971. Some effects of salinity and temperature on early development of Pacific herring (*Clupea pallasii*). *Journal of the Fisheries Research Board of Canada* 28:1545-1562.
- Barrionuevo, W.R., and W.W. Burggen. 1999. O₂ consumption and heart rate in developing zebrafish (*Danio rerio*): influence of temperature and ambient O₂. *American Physiological Society* 276:R505-R513.
- Baumann, H., and D.O. Conover. 2011. Adaptation to climate change: contrasting patterns of thermal-reaction-norm evolution in Pacific versus Atlantic silversides. *Proceedings of The Royal Society B* 278:2265-2273.
- Baumann, H., S. C. Talmage, and C. J. Gobler. 2011. Reduced early life growth and survival in a fish in direct response to increased carbon dioxide. *Nature Climate Change* 2:38-41.
- Baumann, H.S., and E.M. Smith. 2018. Quantifying metabolically driven pH and oxygen

- fluctuations in US nearshore habitats at diel to interannual time scales. *Estuaries and Coasts* 41:1101-1117.
- Beer, S., and J. Rehnberg. 1997. The acquisition of inorganic carbon by the seagrass *Zostera marina*. *Aquatic Botany* 56:277–283.
- Busch, D.S., C.J. Harvey, and P. McElhany. 2013. Potential impacts of ocean acidification on the Puget Sound food web. *ICES Journal of Marine Science* 70(4):823-833.
- Caldeira, K., and M. E. Wickett. 2003. Anthropogenic carbon and ocean pH. *Nature* 423:365.
- Calvo, J., and I.A. Johnston. 1992. Influence of rearing temperature on the distribution of muscle fiber types in the turbot *Scophthalmus maximus* at metamorphosis. *Journal of Experimental Marine Biology and Ecology* 161:45-55.
- Crain, C. M., K. Kroeker, and B. S. Halpern. 2008. Interactive and cumulative effects of multiple human stressors in marine systems. *Ecology Letters* 11:1305-1315.
- Dahlke, F.T., E. Leo, F. C. Mark, H.O. Pörtner, U. Bickmeyer, S. Frickenhaus, and D. Storch. 2016. Effects of ocean acidification increase embryonic sensitivity to thermal extremes in Atlantic cod, *Gadus morhua*. *Global Change Biology* 23(4) 1499-1510.
- Dalton, M.M, P.W. Mote, and A.K. Snover [Eds.]. 2013. *Climate change in the Northwest: Implications for our landscapes, waters, and communities*. Washington, DC: Island Press.
- Davis, B.E., E.E. Flynn, N.A. Miller, F.A. Nelson., N.A. Fanguie, and A.E. Todgham. 2017. Antarctic emerald rockcod have the capacity to compensate for warming when uncoupled from CO₂-acidification. *Global Change Biology* DOI: 10.1111/GCB.13987
- Deigweiher, K., N. Koschnick, H. O. Pörtner, and M. Lucassen. 2008. Acclimation of ion regulatory capacities in gills of marine fish under environmental hypercapnia. *American Journal of Physiology – Regulatory, Integrative and Comparative Physiology* 295:R1660-R1670.
- Deigweiher, K., T. Hirse, C. Bock, M. Lucassen, H.O. Pörtner. 2010. Hypercapnia induced shifts in gill energy budgets of Antarctic notothenioids. *Journal of Comparative Physiology B* 180:347-359.
- Dickson A. G., C. L. Sabine, and J. R. Christian. 2007. *Guide to best practices for ocean CO₂ measurements*. PICES Special Publication 3:1-191.
- Dinnel, P. A., D. P. Middaugh, N. T. Schwarck, H. M. Farren, R. K. Haley, R. A. Hoover, J. Elphick, K. Tobiason, and R. R. Marshall. 2010. Methods for conducting bioassays using embryos and larvae of Pacific herring (*Clupea pallasii*). *Archives of Environmental Contamination and Toxicology* doi 10.1007/s00244-010-9600-8.

- Di Santo, V. 2014. Ocean acidification exacerbates the impacts of global warming on embryonic little skate, *Leucoraja erinacea* (Mitchill). *Journal of Experimental Marine Biology and Ecology* 463:72-78.
- Doney, S. C., V. J. Fabry, R. A. Feely, and J. A. Kleypas. 2009. Ocean acidification: the other CO₂ problem. *Annual Review of Marine Science* 1:169-192.
- Doney, S. C., M. Ruckelshaus, J. E. Duffy, J. P. Barry, and F. Chan, et al. 2012. Climate change impacts on marine ecosystems. *Annual Review of Marine Science* 4:11-37.
- Duarte, C.M., Hendriks, I.E., Moore, T.S., Olsen, Y.S., Steckbauer, A., Ramajo, L., Carstensen, J., Trotter, J.A., McCulloch, M., 2013. Is Ocean Acidification an Open-Ocean Syndrome? Understanding Anthropogenic Impacts on Seawater pH. *Estuaries Coasts* 36, 221–236. doi:10.1007/s12237-013-9594-3.
- Ern, R., and A. J. Esbaugh. 2016. Hyperventilation and blood acid-base balance in hypercapnia exposed red drum (*Sciaenops ocellatus*). *Journal of Comparative Physiology B*. 186:447-460.
- Esbaugh, A. J., Heuer, R., and Grosell, M. 2012. Impacts of ocean acidification on respiratory gas exchange and acid-base balance in a marine teleost, *Opsanus beta*. *Journal of Comparative Physiology B*. 182:921-934.
- Evans, D.H., P.M. Piermarini, and K.P. Choe. 2005. The multifunctional fish gill: Dominant site of gas exchange, osmoregulation, acid-base regulation, and excretion of nitrogenous waste. *Physiological Review* 85:97-177.
- Farrell, A.P., S.G. Hinch, S.J. Cooke, D.A. Patterson, G.T. Crossin, et al. 2008. Pacific salmon in hot water: applying aerobic scope models and biotelemetry to predict the success of spawning migrations. *Physiological and Biochemical Zoology* 8(16) doi:10.1086/592057.
- Feely, R.A., C. L. Sabine, J. M. Hernandez-Ayon, D. Ianson, B. Hales. 2008. Evidence for upwelling of corrosive “acidified” water onto the continental shelf. *Science* 320:1490-1492.
- Feely, R.A., S.C. Doney, and S.R. Cooley. 2009. Ocean acidification: Present conditions and future changes in a high-CO₂ world. *Oceanography* 22(4):36-47.
- Feely, R.A., S. R. Alin, J. Newton, C. L. Sabine, M. Warner, A. Devol, C. Krembs, and C. Maloy. 2010. The combined effects of ocean acidification, mixing, and respiration on pH and carbonate saturation in an urbanized estuary. *Estuarine, Coastal and Shelf Science* 88:442-449.
- Flynn, E.E., B.E. Bjelde, N.A. Miller, and A.E. Todgham. 2015. Ocean acidification exerts negative effects during warming conditions in a developing Antarctic fish. *Conservation Physiology* 3(1): cov033;doi:10.1093/conphys/cov033.

- Franke, A., and C. Clemmesen. 2011. Effects of ocean acidification on early life stages of Atlantic herring (*Clupea harengus* L.). *Biogeosciences* 8:1545-1562.
- Francis, T., and D. Lowry. 2017. Salish Sea Herring Recovery Workshop. Puget Sound Institute, the Washington Department of Fish and Wildlife, and the Salish Sea Studies Institute. Bellingham, WA.
- Frommel, A. Y., R. Maneja, D. Lowe, A. M. Malzahn, A. J. Geffen, A. Folkvord, U. Piatkowski, T. B. H. Reusch, and C. Clemmesen. 2011. Severe tissue damage in Atlantic cod larvae under increasing ocean acidification. *Nature Climate Change* doi:10.1038/NCLIMATE1324.
- Frommel, A.Y., R. Maneja, D. Lowe, C.K. Pascoe, A.J. Geffen, et al. 2014. Organ damage in Atlantic herring larvae as a result of ocean acidification. *Ecological Applications* 24(5):1131-1143.
- Fukuhara, O. 1990. Effect of temperature on yolk utilization, initial growth and behavior of fed and unfed marine fish-larvae. *Marine Biology* 106:169-174.
- Galloway, T.F., E. Kjørsvik, and H. Kryvi. 1998. Effect of temperature on viability and axial muscle development in embryos and yolk sac larvae of the Northeast Arctic cod (*Gadus morhua*). *Marine Biology* 132:559-567.
- Geffen, A.J. 2002. Length of herring larvae in relation to age and time of hatching. *Journal of Fish Biology*. 60:479-485.
- Green, B. S., and R. Fisher. 2004. Temperature influences swimming speed, growth, and larval duration in coral reef fish larvae. *Journal of Experimental Marine Biology and Ecology* 229:115-132.
- Gutowska, M.A., and F. Melzner. 2009. Abiotic conditions in cephalopod (*Sepia officinalis*) eggs: embryonic development at low pH and high $p\text{CO}_2$. *Marine Biology* 156:515-519.
- Hamilton, S.L., C.A. Logan, H.W. Fennie, S.M. Sogard, J.P. Barry, A.D. Makukhov, L.R. Tobosa, K. Boyer, C.F. Lovera, and G. Bernardi. 2017. Species-specific responses of juvenile rockfish to elevated $p\text{CO}_2$: From behavior to genomics. *PLoS ONE* 12(1):e0169670.doi:10.1371/journal.pone.0169670.
- Harley, C. D. G., A. R. Hughes, K. M. Hultgren, B. G. Miner, C. J. B. Sorte, C. S. Thornber, L. F. Rodriguez, L. Tomanek, and S. L. Williams. 2006. The impacts of climate change in coastal marine systems. *Ecology Letters* 9:228-241.
- Haslob, H., H. Hauss, C. Petereit, C. Clemmesen, G. Kraus, M.A. Peck. 2012. Temperature effects on vital rates of different life stages and implications for population growth of Baltic sprat. *Marine Biology* 159:2621-2632.

- Hurst, T. P., E. R. Fernandez, and J. T. Mathis. 2013. Effects of ocean acidification on hatch size and larval growth of walleye Pollock (*Theragra chalcogramma*). *ICES Journal of Marine Science* 70:812-822.
- Hurst, T. P., B. J. Laurel, J. T. Mathis, and L. R. Tobosa. 2014. Effects of elevated CO₂ levels on eggs and larvae of a North Pacific flatfish. *ICES Journal of Marine Science* doi:10.1093/icesjms/fsv050.
- Heuer, R. M., and M. Grosell. 2014. Physiological impacts of elevated carbon dioxide and ocean acidification on fish. *American Journal of Physiology – Regulatory, Integrative and Comparative Physiology* 307:R1061-R1084.
- Hofmann, G. E., J. P. Barry, P. J. Edmunds, R. D. Gates, and D. A. Hutchins, et al. 2010. The effect of ocean acidification on calcifying organisms in marine ecosystems: an organism to ecosystem perspective. *Annual Review of Ecology, Evolution, and Systematics* 41:127-147.
- Hofmann, G.E., and A.E. Todgham. 2010. Living in the now: physiological mechanisms to tolerate a rapidly changing environment. *Annual Review of Physiology* 72:127-145.
- Hofmann, G.E., J.E. Smith, K.S. Johnson, U. Send, L.A. Levin, et al. 2011. High-Frequency Dynamics of Ocean pH: A Multi-Ecosystem Comparison. *PLoS ONE* 6(12): e28983. doi:10.1371/journal.pone.0028983.
- IPCC. 2014. Long-term climate change: projections, commitments and irreversibility. In *climate change 2013, synthesis report*, Cambridge, UK: Cambridge University Press.
- Ishimatsu, A., T. Kikkawa, M. Hayashi, K. S. Lee, and J. Kita. 2004. Effects of CO₂ on marine fish: larvae and adults. *Journal of Oceanography* 60:731-741.
- Ishimatsu, A., M. Hayashi, T. Kikkawa. 2008. Fishes in high-CO₂, acidified oceans. *Marine Ecology Progress Series* 373:295-302.
- Johansen, J.L., and G.P. Jones. 2011. Increasing ocean temperature reduces the metabolic performance and swimming ability of coral reef damselfishes. *Global Change Biology* 17:2971-2979, doi:10.1111/j.1365-2486.2011.02436.x.
- Johnston, I. A. 1993. Temperature influences muscle differentiation and the relative timing of organogenesis in herring (*Clupea harengus*) larvae. *Marine Biology* 116:363-379.
- Johnston, I.A., N.J. Cole, M. Abercromby, and V.L.A. Vieira. 1998. Embryonic temperature modulates muscle growth characteristics in larval and juvenile herring. *The Journal of Experimental Biology* 201:623-646.
- Johnston, I.A., V.L.A. Vieira, and G.K. Temple. 2001. Functional consequences and population differences in the developmental plasticity of muscle to temperature in Atlantic herring

- Clupea harengus*. Marine Ecology Progress Series 213:285-300.
- Kawakami, T., H. Okouchi, M. Aritaki, J. Aoyama, and K. Tsukamoto. 2011. Embryonic development and morphology of eggs and newly hatched larvae of Pacific herring (*Clupea pallasii*). Fisheries Science 77:183-190.
- Kikkawa, T., A. Ishimatsu, and J. Kita. 2003. Acute CO₂ tolerance during the early developmental stages of fur marine teleosts. DOI 10.1002/tox.10139
- Kroeker, K. J., R. L. Kordas, R. N. Crim, and G. G. Singh. 2010. Meta-analysis reveals negative yet variable effects of ocean acidification on marine organisms. Ecology Letters 13:1419-1434.
- Laakkonen, H.M., P. Strelkov, D.L. Lajus, and R. Väinölä. 2015. Introgressive hybridization between the Atlantic and Pacific herrings (*Clupea harengus* and *C. pallasii*) in the north of Europe. Marine Biology 16:36-54.
- Lassuy, D.R. 1989. Species Profiles: life histories and environmental requirements of coastal fishes and invertebrates (Pacific Northwest) – Pacific herring. U.S. Fish Wildl. Serv. Biol. Rep. 82(11.126) U.S. Army Corps of Engineers, TR-EL-82-4.
- Lefevre, S. 2016. Are global warming and ocean acidification conspiring against marine ectotherms? A meta-analysis of the respiratory effects of elevated temperature, high CO₂ and their interaction. Conservation Physiology 4(1):cow009;doi:10.1093/conphys/cow009.
- Lenarz, W.H., R.J. Larson, S. Ralston. 1991. Depth distributions of late larvae and pelagic juveniles of some fishes of the California Current. California Cooperative Oceanic Fisheries 32:41-46.
- Maneja, R.H., R. Dienshrum, V. Thiyagarajan, A.B. Skiftesvik, A.Y. Frommel, et al. 2014. The proteome of Atlantic herring (*Clupea harengus* L.) larvae is resistant to elevated pCO₂. Marine Pollution Bulletin 86:154-160.
- McLaskey, A.K., J.E. Keister, P. McElhany, and M.B. Olson. 2016. Development of *Euphausia pacifica* (krill) larvae is impaired under pCO₂ levels currently observed in the Northeast Pacific. Marine Ecology Progress Series 555:65-78.
- Melzner, F., M.A. Gutowska, M. Langenbuch, S. Dupont, M. Lucassen, M.C. Thorndyke, M. Bleich, and H.O. Pörtner. 2009. Physiological basis for high CO₂ tolerance in marine ectothermic animals: pre-adaptation through lifestyle and ontogeny? Biogeosciences 6:1-9.
- Miller, G. M., F. J. Kroon, S. Metcalfe, and P. L. Munday. 2015. Temperature is the evil twin: effects of increased temperature and ocean acidification on reproduction in a reef fish. Ecological Society of America 25:603-620.

- Miller, C.A., S. Yang, and B.A. Love. 2017. Moderate increase in TCO₂ enhances photosynthesis of seagrass *Zostera japonica*, but not *Zostera marina*: Implications for acidification mitigation. *Frontiers in Marine Science* 4:228.
Doi:10.3389/fmars.2017.00228.
- Mirkovic, T., and P. Rombough. 1997. The Effect of Body Mass and Temperature on the Heart Rate, Stroke Volume, and Cardiac Output of Larvae of the Rainbow Trout, *Oncorhynchus mykiss*. *Physiological Zoology* 71(2):191-197.
- Moran, A.L., and H. A. Woods. 2010. Limits to diffusive O₂ transport: Flow, form, and function in nudibranch egg masses from temperate and polar regions. *PLoS ONE* 5(8):e12113. doi:10.1371/journal.pone.0012113.
- Munday, P. L., D. L. Dixon, J. M. Donelson, G. P. Jones, M. S. Pratchett, G. B. Devitsina, and K. B. Døving. 2008a. Ocean acidification impairs olfactory discrimination and homing ability of a marine fish. *PNAS* 106:1848–1852.
- Murray, J.W., E. Roberts, E. Howard, M. O'Donnell, C. Bantam, et al. 2015. An inland sea high nitrate-low chlorophyll (HNLC) region with naturally high pCO₂. *Limnology and Oceanography* 60:957-966.
- Nissling, A. 2004. Effects of temperature on egg and larval survival of cod (*Gadus morhua*) and sprat (*Sprattus sprattus*) in the Baltic Sea – implications for stock development. *Hydrobiologia* 514:115-123.
- NOAA National Centers for Environmental Information (NCEI). Water Temperature Table of the Northern Pacific Coast. Data accessed from the NOAA NCEI website:
<https://www.nodc.noaa.gov/dsdt/cwtg/npac.html>.
- Pacella, S.R., C.A. Brown, G.G. Waldbusser, R.G. Labiosa, and B. Hales. 2018. Seagrass habitat metabolism increases short-term extremes and long-term offset of CO₂ under future ocean acidification. *PNAS* 115(15):3870-3875.
- Peck, M.A., and L.J. Buckley. 2008. Measurements of larval Atlantic cod (*Gadus morhua*) routine metabolism: temperature effects, diel differences and individual-based modeling. *Journal of Applied Ichthyology* 24:144-149.
- Peck, M.A., P. Kanstinger, L. Holste, and M. Martin. 2012. Thermal windows supporting survival of the earliest life stages of Baltic herring (*Clupea harengus*). *ICES Journal of Marine Science* 69(4):529-536.
- Peck, M.A., and M. Moyano. 2016. Measuring respiration rates in marine fish larvae: challenges and advances. *Journal of Fish Biology* 88:173-205.
- Perry, S.F., and K.M. Gilmour. 2006. Acid-base balance and CO₂ excretion in fish: Unanswered

- questions and emerging models. *Respiratory Physiology and Neurobiology* 154:199-215.
- Pimentel, M.S., F. Faleiro, G. Dionísio, T. Repolho, P. Pousão-Ferreira, J. Machado, and R. Rosa. 2014. Defective skeletogenesis and oversized otoliths in fish early stages in a changing ocean. *The Journal of Experimental Biology* 217:2062-2070.
- Pörtner, H.O. 2001. Climate change and temperature-dependent biogeography: oxygen limitation of thermal tolerance in animals. *Naturwissenschaften* 88:137-146.
- Pörtner, H.O., M. Langenbuch, and A. Reipschläger. 2004. Biological impacts of elevated ocean CO₂ concentrations: Lessons from animal physiology and earth history. *Journal of Oceanography* 60:705-718.
- Pörtner, H.O., M. Langenbuch, and B. Michaelidis. 2005. Synergistic effects of temperature extremes, hypoxia, and increases in CO₂ on marine animals: From Earth history to global change. *Journal of Geophysical Research* 110(CO9S10):doi 10.1029/2004JC002561.
- Pörtner, H.O. 2008. Ecosystem effects of ocean acidification in times of ocean warming: a physiologist's view. *Marine Ecology Progress Series* 373:203-217.
- Pörtner, H.O., C. Bock, R. Knust, G. Lannig, M. Lucassen, et al. 2008. Cod and climate in a latitudinal cline: physiological analyses of climate effects in marine fishes. *Climate Research* 37:253-270.
- Pörtner, H.O., and A.P. Farrell. 2008. Physiology and climate change. *Science* 322(5902):690-692.
- Pörtner, H.O., and R. Knust. 2007. Climate change affects marine fishes through the oxygen limitation of thermal tolerance. *Science* 315:95-97.
- Pörtner, H.O. 2012. Integrating climate-related stressor effects on marine organisms: unifying principles linking molecule to ecosystem-level changes. *Marine Ecology Progress Series* 470:273-290.
- Purcell, J.E., D. Grosse, and J.J. Grover. 1990. Mass abundances of abnormal Pacific herring larvae at a spawning ground in British Columbia. *Transactions of the American Fisheries Society* 119:3, 463-469.
- Reum, J. C. P., S. R. Alin, R. A. Feely, J. Newton, M. Warner, and P. McElhany. 2014. Seasonal carbonate chemistry covariation with temperature, oxygen, and salinity in a fjord estuary: implications for the design of ocean acidification experiments. *PLOS ONE* e89619. doi:10.1371/journal.pone.0089619.
- Rombough, P.J., 1997. The effects of temperature on embryonic and larval development. In: *Global Warming. Implications for Freshwater and Marine Fisheries*. C.M. Wood and D.G. McDonald, (Eds.). Cambridge University, Press Cambridge, pp: 177-223.

- Sabine, C.L., R.A. Feely, N. Gruber, R.M. Key, K. Lee, et al. 2004. The oceanic sink for Anthropogenic CO₂. *Science* 305:367-371.
- Shelton, A. O., T. B. Francis, G. D. Williams, B. Feist, K. Stick, and P. S. Levin. 2014. Habitat limitation and spatial variation in Pacific herring egg survival. *Marine Ecology Progress Series* 514:231-245.
- Snyder, J.T., C.S. Murray, and H. Baumann. 2018. Potential for maternal effects on offspring CO₂ sensitivities in the Atlantic silverside (*Menidia menidia*). *Journal of Experimental Marine Biology and Ecology* 499:1-8.
- Sswat, M., M.H. Stiasny, F. Jutfelt, U. Riebesell, C. Clemmesen. 2018a. Growth performance and survival of larval Atlantic herring, under the combined effects of elevated temperatures and CO₂. *PLoS ONE* 13(1):e0191947
- Sswat, M., M.H. Stiasny, J. Taucher, M. Algueró-Muñiz, L.T. Bach, et al. 2018b. Food web changes under ocean acidification promote herring larvae survival. *Nature Ecology and Evolution* doi:10.1038/s41559-018-0514-6.
- Stick, K. C., and A. Lindquist. 2009. Washington state herring stock status report. FPA 09-05:1-111.
- Stick, K.C., A. Lindquist, and D. Lowry. 2014. 2012 Washington state herring stock status report. Washington Department of Fish and Wildlife, Fish Program Technical Report No. FPA 14-09.
- Sullivan, C. A. 2013. Carbonate chemistry in the San Juan channel: Characterization and suggestions for mitigation. Masters Thesis. School of Marine and Environmental Affairs. University of Washington.
- Sunda, W.G., and W.J. Cai. 2012. Eutrophication induced CO₂-acidification of subsurface coastal waters: interactive effects of temperature, salinity, and atmospheric pCO₂. *Environmental Science and Technology* 46(19): 10651-10659.
- Thomsen, J., M.A. Gutowska, J. Saphörster, A. Heinemann, K. Trübenbach, et al. 2010. Calcifying invertebrates succeed in a naturally CO₂-rich coastal habitat but are threatened by high levels of future acidification. *Biogeosciences* 7:3879-3891.
- Truchot, J. P., and A. Duhameljouve. 1980. Oxygen and carbon-dioxide in the marine inter-tidal environment – diurnal and tidal changes in rockpools. *Respiration Physiology* 39:241–254.
- United Nations Human Settlements Programme. 2011. Cities and climate change: global report on human settlements. Earthscan, London.

Unsworth, R.K.F., C. J. Collier, G. M. Henderson, and L. J. McKenzie. 2012. Tropical seagrass 55 meadows modify seawater carbon chemistry: implications for coral reefs impacted by ocean acidification. *Environmental Research Letters* 7:024026.

Venn, A.A., E. Tambutté, M. Holcomb, J. Laurent, and D. Allemand, et al. 2013. Impact of seawater acidification on pH at the tissue-skeleton interface and calcification in reef corals. *PNAS* 110(5):1634-1639.

Vieira, V. I., and I. A. Johnston. 1992. Influence of temperature on muscle-fibre development in larvae of the herring *Clupea harangus*. *Marine Biology* 112:333-341.

WDFW. 2011. Pacific Herring Information Summary [https://wdfw.wa.gov/conservation/research/projects/marine_fish_monitoring/herring_population_assessment/].

Wittmann, A.C., and H.O. Pörtner. 2013. Sensitivities of extant animal taxa to ocean acidification. *Nature Climate Change* 3:995-1001.

Wotton, J.T., C.A. Pfister, and J.D. Forester. 2008. Dynamic patterns and ecological impacts of declining ocean pH in a high-resolution multi-year dataset. *PNAS* 105(48):18848-18853.

Appendix A

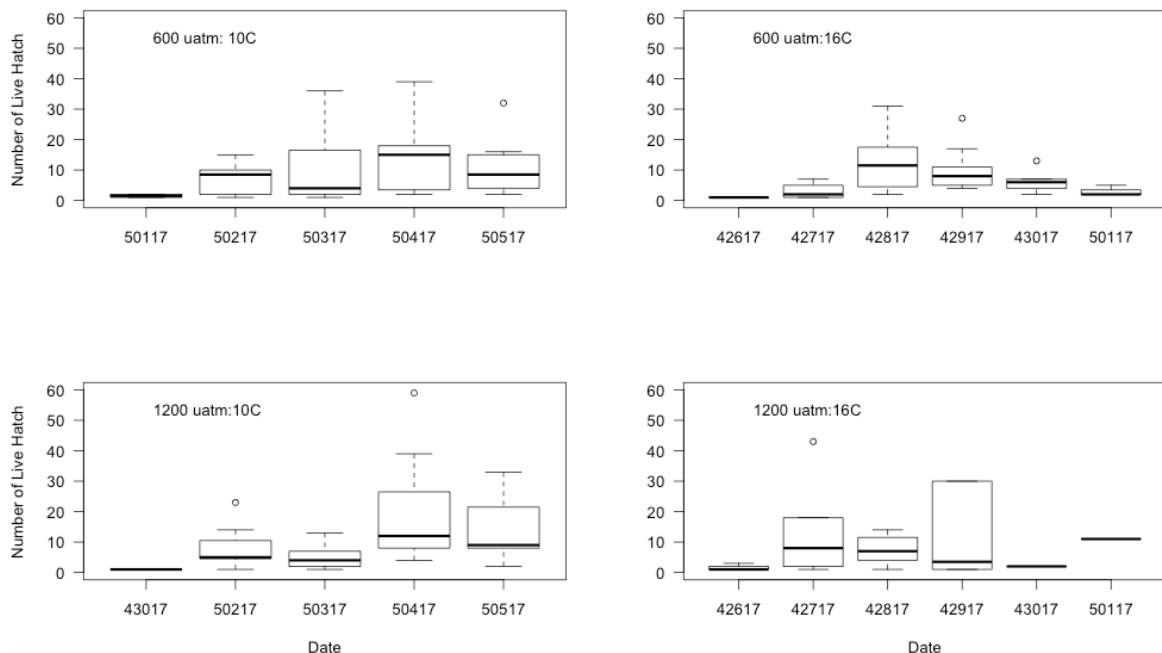


Figure A1: Mean live-hatched Pacific herring larvae during each hatching day for 600:12 (n = 313), 600:16 (n = 240), 1200:10 (n = 302), and 1200:16 (n = 181). Whiskers extending from the boxplots indicate standard deviation (SD) from the median (solid black line). Unfilled circles outside the plots indicate outlying data points from the SD. Treatments are indicated in the upper left corner.

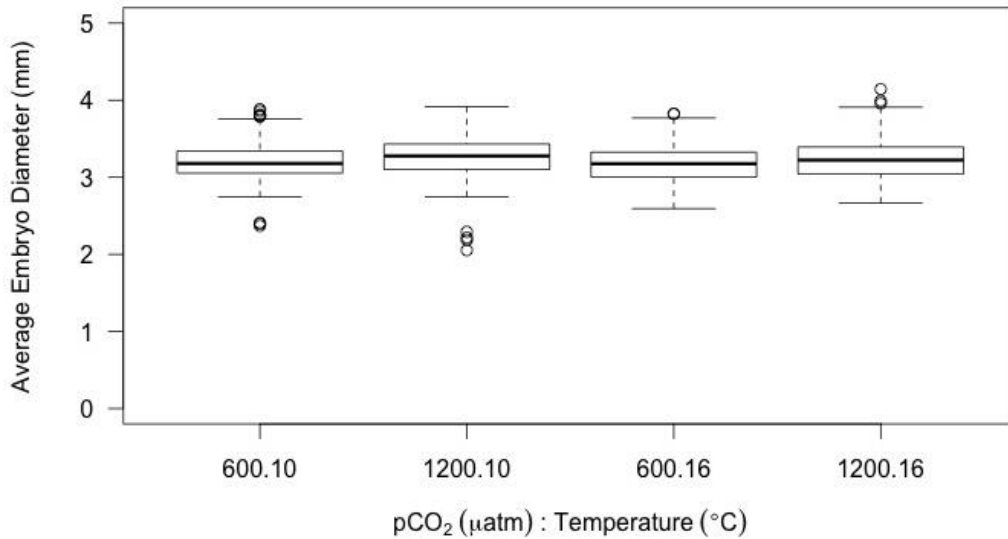


Figure A2: The average Pacific herring embryo diameters as a function of treatment groups were measured from development photos taken during the incubation period.

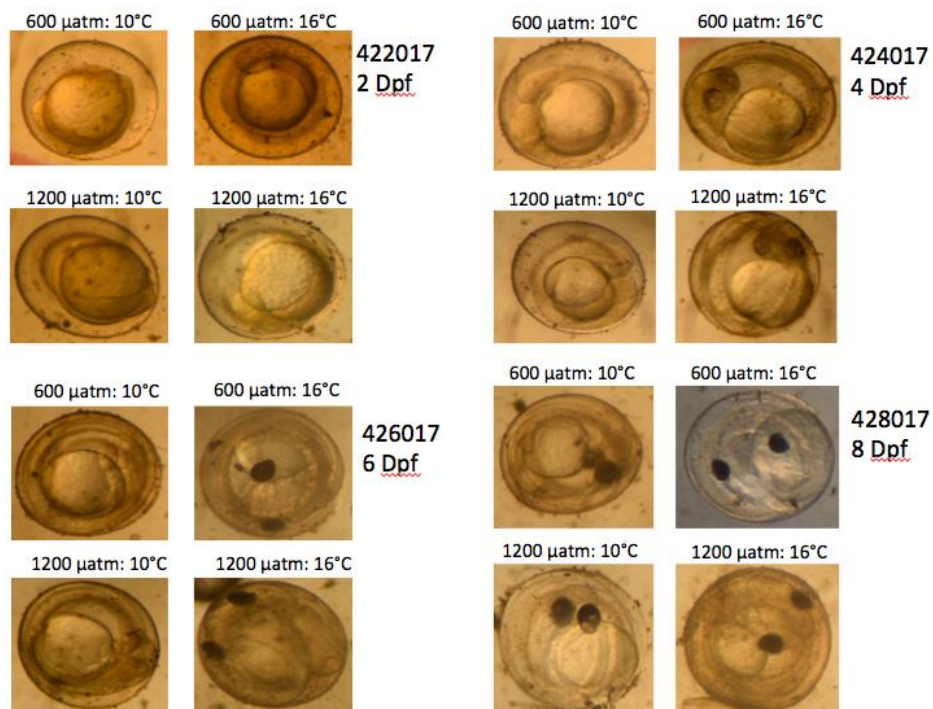


Figure A3: Pacific herring embryo development during incubation. Photos are from 2, 4, 6, and 8 days post-fertilization (dpf).